ANALYSIS OF SHORELINE CHANGE FOR JEKYLL AND SAPELO ISLANDS, GEORGIA WITH GIS TECHNIQUES

by

BEI TU

Under the Direction of E. Lynn Usery

ABSTRACT

The objective of this research is to use geographic information systems (GIS) to quantify shoreline position change during 1954 and 1999 for Sapelo Island and Jekyll Island in Georgia, USA. Shorelines from multiple years were manually traced from digital raster graphics, aerial photographs, digital orthophoto quad quadrangles and a lidar image using ArcView GIS software, Version 3.3. This study showed that the northern ends of Jekyll and Sapelo islands are eroding, whereas the southern ends are accreting. Mann-Whitney test (two-tailed) indicated that the mean accretion rates and annual change rates (regardless of direction) of the two islands differed statistically during 1954-1974,1974-1993 and 1954-1999. The mean recession rates were significantly different during 1954-1974 and 1974-1993, but not so for 1954-1999. Human activity exerted a heavy influence on the shoreline change. Quantifying shoreline change provides useful data on the effects of engineering structures on erosion and is important for coastal zone management and planning.

INDEX WORDS: GIS, shoreline change, Sapelo Island, Jekyll Island, lidar, coastal zone

ANALYSIS OF SHORELINE CHANGE FOR JEKYLL AND SAPELO ISLANDS, GEORGIA WITH GIS TECHNIQUES

by

BEI TU

B.E., Wuhan University, P. R. China, 2001

A Thesis Submitted to the Graduate Faculty of The University of Georgia in Partial Fulfillment of the Requirements for the Degree

MASTER OF SCIENCE

ATHENS, GEORGIA

2004

ANALYSIS OF SHORELINE CHANGE FOR JEKYLL AND SAPELO ISLANDS, GEORGIA WITH GIS TECHNIQUES

by

BEI TU

Major Professor: E. Lynn Usery

Committee: David S. Leigh
Marguerite Madden

Electronic Version Approved:

Maureen Grasso
Dean of the Graduate School
The University of Georgia
August 2004

DEDICATION

This is dedicated to my dear parents for their unconditional love and support to me.

ACKNOWLEDGEMENTS

So many people have helped me in this study directly or indirectly. Although I am thankful to all, I cannot hope to give all the credit that is due. My deepest gratitude goes to my major professor, Dr. Lynn Usery, for his inspiration, invaluable advice and excellent guidance. Without his direction and help along the way the completion of my thesis would have been impossible. I would like to thank Dr. Marguerite Madden for her generous help. Her insightful suggestions always inspired me to work further on this project. My sincere appreciation also goes to Dr. David Leigh; our discussions provided me with a better understanding of the topic. I want to thank Dr. Keqi Zhang at at the Florida International University for allowing me to use the Metric Mapping ArcView extension developed by him. I appreciate the help from my good friend Roy Fenoff on my field trip to Jekyll Island.

I am genuinely grateful to my family for their unconditional love, support and always being there for me. I want to thank my best friend, Amanda Jones, for her encouragements, prayers and confidence in me, and above all, for her precious friendship. Last but not least, I am thankful to God for all his blessings in my life.

TABLE OF CONTENTS

Page

LIST OF TABLES

Page

LIST OF FIGURES

Page

CHAPTER 1

INTRODUCTION

The immediate coastal environment may be defined as the narrow zone of interaction between land and ocean, which may consist of barrier islands (White and Wang, 2002). The definition of a shoreline or coastline, as they are used interchangeably in this research, is the physical interface of land and water. Detection and measurement of coastline changes are of great importance in environmental studies as the shoreline status is crucial to humans, wildlife and estate properties of these areas. Shoreline variations have a direct impact on economic development and land management (Chen and Rau, 1998). Such information is necessary for coastal development to be designed and constructed with adequate safety and in the most economical manner (Stafford and Langfelder, 1971).

As defined by the International Geosphere Biosphere Programme, the coastal zone is the whole region from the 200-m bathymetric contour at sea to the 200-m elevation contour on the land (Coastal Georgia Regional Development Center, 2004). Across the United States, approximately 53% of the population lives within the coastal zone that comprises only 18% of the nation's total land area. Indeed, many man-made facilities are located at elevations less than 3 m above sea level. Coastal populations in the United States are projected to reach 127 million people by the year 2010. Because the dense population and fast development in the coastal regions, terrain changes in coastal areas have attracted worldwide interest (Welch *et al.* 1992, Stokkom *et al.* 1993).

The Georgia Bight extends roughly 1,200 km between Cape Hatteras, North Carolina and Cape Canaveral, Florida. Coastal research on the apex of the Georgia Bight expanded rapidly

beginning in the 1960s, peaked in the 1970s and 1980s, and experienced a decline during the 1990s (Taylor *et al.* 1995). Previous studies provided a general understanding of erosion patterns around the barrier islands, but were limited in quality and lacked quantifying information due to data constraints and technology limits at the time of the research. Common sources for shoreline data include U.S. Geological Survey (USGS) quadrangle maps, aerial photographs, nautical charts and beach profiles. In recently years, satellite images, radar and LIght Detection and Ranging (lidar) data have become more available with the advent of new sensors, which allow for a much more accurate shoreline change analysis. Because the coastal processes are complex and mutually interdependent, it is difficult to comprehensively evaluate the factors that affect coastline change. In a general sense, the important elements are the intensity of waves and currents, topography of the continental shelf, tidal range, climate and human-induced influences (Inman and Brush, 1973)

A chain of barrier islands in Georgia stretches over 160 km from northernmost Tybee Island near the South Carolina border to Cumberland Island near the Florida border. Four of Georgia's 14 major barrier islands are commercially developed, namely Tybee, St. Simon's, Sea Island and Jekyll Island; the remaining 10 islands are in relatively undeveloped states being preserved by either public or private initiative. Historical rates of shoreline change for Georgia's coastline are lacking in quantity and quality (Foyle, 2000). This research is designed to obtain statistically valid information on the directions and rates of coastline change; compare the change patterns of the developed island to the undeveloped island to evaluate the influence of human activities. Hence, this study will fill an existing knowledge void for the Georgia coast. The primary objective of this project is to accurately quantify and compare shoreline change of Jekyll Island and Sapelo Island between the1950s and 1990s using a geographic information

systems (GIS) with the aid of a variety of remotely sensed data and statistical methods. The secondary objective is to investigate several possible factors causing differences in shoreline changes between the two islands. In this research, coastline positions and change patterns of these two islands during 1954-1974, 1974-1993 and 1954-1999 were examined. These dates were chosen due to data availability. Annual erosion, accretion and average shoreline change rates (regardless of direction) of the two islands during the time of study were calculated and compared to see if they differed statistically. Several possible factors causing differences in coastal processes of the study area were briefly evaluated. Multiple data sets used in this research include USGS Digital Raster Graphics (DRG), vertical aerial photographs, Digital Orthophoto Quad Quadrangles (DOQQ) and lidar images.

Following a review of previous coastal studies, shoreline mapping techniques and shoreline change rate computation techniques in chapter two, chapter three will introduce the study sites and data sources. Chapter four presents the methodology, and results and conclusion will be discussed in chapter five and six.

CHAPTER 2

LITERATURE REVIEW

2.1 Previous Coastal Studies

Methods for detecting shoreline changes can be divided into three major categories: ground surveying, image measurement and modern altimetric technology (Chen and Rau, 1998). Ground surveying is time consuming and labor intensive, but high accuracy is possible. Remote sensing has been less successful in the coastal zone than in the other areas due to the problem of scale (Cracknell, 1999). The main difficulty in extraction of shorelines results from the dynamic behavior of water-land boundaries that vary according to the time-dependent tidal elevations. The combined effect of change over time and space makes the analysis complicated. For image measurement, there are two major sources of remotely sensed imagery: airborne photographs and satellite images.

Vertical aerial photographs are a well-established source of information for coastal studies. Interpretation of aerial photographs as a technique for detecting shoreline change began in the late 1960's (Anders *et al.* 1991). An aerial photograph captures a large amount of ground features along a coastline that exist at the time of photography. The advantage of sequential aerial photography is in providing long-term shoreline change trends (Ashry and Wanless, 1967). Stafford and Langfelder (1971) evaluated a procedure of using sequential aerial photographs to study North Carolina coastline change between 1938 and 1966. Stable reference points were selected on the photographs from multiple years, and the distance between these points and points on the dune line and High Water Line (HWL) were then measured. The obtained

measurements were multiplied by the scale of the aerial photographs to produce ground distances. The differences in ground distances represent the distance of shoreline movement during the time interval. It concluded that although the value of shoreline change at a particular reference point may consist substantial error, the mean distance of change over a section of shoreline is not affected appreciably. However, it did evaluate the composite error in a quantitative manner. Dolan *et al.* (1979) tested using aerial photographs and an orthogonal grid mapping system to examine shoreline change. They concluded that the total measurement error is potentially as much as 25 m for the distance of change. It means that for a time interval of 25 years, change rates of less than 1 m per year are within the range of inaccuracy and must be applied with caution.

Carter (1978) investigated the applicability of satellite images for data collection on wetlands. Not much could be done with the Landsat MSS data of 80-m spatial resolution for most estuaries, as objects that were smaller then 80 m could not be distinguished by the sensor at that time. This is not the case today, for example, Landsat 7 has a panchromatic band with 15-m spatial resolution. Wang and Koopmans (1993) used near IR images to detect shorelines. In their research, profile gradients were analyzed to determine the shoreline. Recently a number of investigations have been reported on shoreline extraction from optical images. In Frihy *et al*. (1994) change detection of the northeastern Nile Delta of Egypt, Landsat satellite image data were utilized together with a series of topographic maps to cover an 86-year monitoring period. Chen *et al.* (1995) reported a zero-order approach, detecting shoreline changes on the west coast of Taiwan. In this approach, two SPOT images sampled at two instances were compared directly when the two images have similar tidal elevations. This approach is easy to implement, however, two images acquired with similar tidal elevations cannot always be expected in reality.

With the availability of all-weather sensors, such as synthetic aperture radar (SAR), combining optical and SAR images provides a sound basis for analyzing the dynamic shoreline behavior. Chen and Shyu (1998) proposed an original scheme for automated extraction of shorelines from optical and SAR images. This approach includes first obtaining a rough land-water boundary and then refining the separation by edge detection and edge tracing algorithms. Experimental results indicate that the accuracy of the extracted shorelines is within 1.5 pixels. These results provide a reliable basis for shoreline change analysis in the tideland area when multi-temporal images and tidal measurements are available. Chen and Rau (1998) presented a novel approach to detect shoreline changes that uses multi-temporal satellite images and tidal measurements based on previous research (Chen and Shyu, 1998). The scheme is composed of two major components. The first is the reconstruction of a reference digital terrain model (DTM) from a set of reference SPOT images and tidal measurements. The second part involves tracing the shoreline from the reference DTM. Then, the shoreline is compared with its counterpart from a historical satellite image. Experimental results show that the inaccuracy in the measuring area of the test sand barriers ranges between 7.6% and 12.5%.

As the spatial and temporal resolutions of satellite images have significantly improved in recent years, the applicability of the images to coastal zone monitoring has become more promising. Scott *et al.* (2002) demonstrated that Landsat 7 Thematic Mapper data could be used to accurately extract land-water boundaries. The southern Louisiana coastline in the winter of 2000 was classified into land and open water using the ERDAS implementation of the tasseled-cap algorithm. The land-water interface was then traced. Though the 30-m spatial resolution is comparatively low given the dynamic nature of the coastal region, this drawback is compensated by high color resolution, the increased temporal resolution and decreased cost. The land-water

boundary derived from this method is equivalent in accuracy of the vector shoreline published by National Oceanic and Atmospheric Administration (NOAA), and to approach the accuracy of USGS's 1:24,000-scale topographic quadrangles.

The newer altimetric technology, which uses radar altimeters or lasers, has a high potential with these detectors more widely available now. Airborne lidar systems include three major components: a laser ranging unit, an Inertial Measurement Unit (IMU) and a Global Positioning System (GPS) receiver. Lidar uses a transmitted laser beam to measure distance and depict the terrain of the Earth. It determines distance by measuring the time it takes for a light pulse to reflect back from a target to a detector. It is typically flown on aircraft at an altitude between 400 m and 800 m above ground level, and measures topography by combining a scanning laser and GPS receivers. Hence, the achievement of spatial resolution of 50 cm and the vertical resolution of 15 cm or less become possible. Lidar became feasible and popular due to the maturation of two associated technologies: GPS products and IMU (Krabill *et al.* 2000). They allow accurate registration of the lidar data to ground surfaces. Advances in GPS technologies during the last few years, for example, differential GPS, made it possible to locate a GPS receiver within a few centimeters. Inertial measurement unit incorporates highly accurate gyroscopes and accelerometers to monitor the attitude of the aircraft platform, which is important to refine its true location.

White and Wang (2002) analyzed morphologic change in the 70-km stretch of southern North Carolina coastline with a digital elevation model (DEM) derived from lidar data. Between 1997 and 2000, there were four annual lidar data acquisitions over the study area. The high-resolution DEM data make an inclusive quantitative study into the spatial patterns of morphologic change possible. A T-test of net volumetric change per unit area for study areas of

different beach management practices was conducted. Results indicate that the volumetric change is statistically significant when different practices were applied to them (White and Wang, 2002).

2.2 Shoreline Mapping Techniques

A variety of approaches have been developed to extract shoreline change information from maps and aerial photographs. The techniques have evolved from simple direct measurements appropriate for small areas to mechanical and computerized procedures that are capable of utilizing all available sources.

Point Measurement

Point measurement from aerial photographs was widely used to calculate historical rates of shoreline change. This procedure was developed by Stafford (1971) to study coastal erosion along the Outer Banks of North Carolina. The distances between a fixed reference object and the shoreline at various years are measured from multiple aerial photographs. An erosion rate for each point is then computed by dividing the difference between distances to the shoreline from a reference point by the time interval between photographs. Radial distortion and tilt displacement can be minimized by working only at the center of each photograph, but relief displacement cannot be corrected. Though this method is inexpensive, it is not likely to meet the National Map Accuracy Standards (NMAS). In addition, a continuous representation of the coast cannot be obtained.

Orthogonal Grid Mapping System

Dolan *et al*. (1978) developed an orthogonal grid mapping system that can produce a continuous representation of the shoreline. First, 1:5,000 scale base maps of the study area is generated by photo enlargement of a series of 7.5-minute USGS maps. Historical aerial

photographs are then enlarged and superimposed onto the base map, and the coastlines are manually traced using a projecting light table. Shoreline position change is determined by using a rectilinear grid to take measurements at 100-m intervals along the shoreline. This approach does not correct radial distortion, tilt displacement or relief displacement, and does not meet the NMAS.

Stereo Zoom Transfer Scope (ZTS)

Developed by Fisher (1979), this approach was regarded to represent the state-of-the-art in coastal mapping for a period of time. The Stereo Zoom Transfer Scope (ZTS) is efficient in eliminating scale differences by superimposing aerial photography onto a base map and rectification to ground control points (Philipson, 1997). After rectification and adjustment in scale, the shoreline can be traced from a set of aerial photographs. The ZTS method can minimize distortion and tilt displacement but requires time-consuming process. It does not correct displacement due to relief.

Metric Mapping

This semi-automated technique of shoreline mapping, devised by Leatherman (1983), was designed to use the high-speed data processing capabilities of a computer to imitate advanced photogrmmetric techniques. Metric mapping applies an analytical treatment of photogrammetry based on mathematical models and numerical solutions rather than analog methods. Leatherman (1983) defined the metric quality maps as those maps which: 1. are gridded with one of the three standard coordinate systems (State Plane, Latitude and Longitude, or Universal Transverse Mercator), 2. are at suitably large scale, and 3. meet NMAS.

Most prior mapping techniques have drawn on aerial photograph alone as a source material, while metric mapping allows for the collection of shoreline data from all available

sources of accurate information, such as topographic maps, satellite images, radar images, etc. This sophisticated system was developed to allow for the production of accurate maps, using less expensive equipment and less human effort than is required in advanced photogrammetric techniques (Leatherman, 1983). Metric mapping can remove radial distortion and tilt displacement.

ZTS and GIS

McBride *et al.* (1991) presented ZTS and GIS approach to map barrier island changes in Louisiana. This method combines ZTS, computerized design and drafting (CADD), computer cartography and GIS technology. Aerial photographs were registered to USGS 7.5-minute quadrangles using a ZTS. Aerial photographs and topographic sheets produced by the National Ocean Service (NOS) of NOAA were scanned, and shorelines were manually digitized in their original projections, ellipsoids and datum. Digitized shorelines then were transformed to a common projection, datum and coordinate system using computer mapping hardware and software. After conversion, transects were established and average erosion rates were computed. This approach allows the combined utilization of aerial photographs and maps, minimizes the radial and tilt distortion but has no improvement on accuracy compared with previous methods.

GIS Strategy

Hilland *et al.* (1993) devised GIS approach, which combines CADD, computer cartography and GIS software packages. It uses similar procedures for map digitization and conversion as the ZTS and GIS technique. Here, Hilland *et al.* (1993) developed a second method, in addition to using the ZTS, to rectify photographs. First, aerial photographs were scanned and rectified utilizing software with control points from a previously digitized map. The control points are geographic coordinates of labeled grid marks on maps, or features on photos

that can be identified on a map. The shoreline was then digitized as it appears on the computer screen. An Automated Shoreline Analysis Program (ASAP) was used to quantify shoreline change at 50 m intervals. Geographic Information Systems allow for the compilation of shoreline data from all available sources. Given its considerable advantages over traditional analytical techniques, GIS technology is rapidly becoming an integral part of coastal management efforts worldwide.

2.3 Shoreline Change Rate Computation Techniques

All methods used for computing shoreline rate-of-change involve measuring the differences between shoreline positions through time. Methods that have been used include: the end point rate, linear regression, jackknifing and the average of rates. Each of these will be discussed in more details below.

End Point Rate (EPR)

The End Point Rate (EPR) is the simplest approach as it uses only two shoreline positions for the calculation. The coastline change rate is determined by comparison of shoreline positions over time elapsed. The earliest and latest dates are used in Figure 2.1, but given the availability of multiple shoreline positions, combinations of EPRs can be computed.

The main advantages of the EPR approach are the simplicity of computation and its widespread application. Over 75% of the data assembled in a comprehensive United States shoreline information system (CEIS) were computed using the EPR method (Dolan *et al.* 1991). There are two major drawbacks of using EPR to compute shoreline rate-of-change. First, false data can have strong influence on the results as only two data points are used. Second, when data that are available in the record are not incorporated into the analysis, important trends in the position change may be neglected.

Linear Regression (LR)

The objective of the linear regression (LR) approach is to generate a best-fit line, using the technique of least squares, through the entire data set of shoreline positions (Dolan *et al.* 1991). The slope of the best-fit line is an estimate of shoreline rate-of-change as shown in Figure 2.2. This method is based on statistical concepts, requires no priori analysis and is easy to complete. Furthermore, it uses all the available data to compute the rate.

One disadvantage of this approach is that some dates have heavier influence on the regression when the shoreline positions are clustered. For instance, many long-term data sets consist of limited coastline positions from early dates and a cluster of recent positions obtained from aerial photographs or satellite images. Regression lines generated from these data yield rate-of-change that may be imbalanced between the early date and modern dates.

Jackknifing (JK)

The jackknifing method resembles linear regression in that it includes all the data and is purely computational, but the outcome is less subject to the influence of data clusters. Jacknifing uses all possible combinations of LRs provided by omitting one point each iteration, as demonstrated in Figure 2.3. The average slope of this family of best-fit lines is an estimate of the long-term trend. The major disadvantages are extensive computations (Dolan *et al*. 1991).

Average of Rates (AOR)

Foster and Savage (1989) designed this method for computing shoreline rate-of-change along the Florida coast. All possible rates are given by the slopes of a family of EPR lines as illustrated in Figure 2.4. The average of rates is a computation based on the error in the original map or image sources and the longest time period used for EPR method. They used this scheme

to predict future changes based on the most recent trend of coastline change. They advocate AOR to be used in combination with the EPR or LR as a means of verification.

2.4 Important Factors of Shoreline Change

Our coastlines are constantly retreating or advancing. The causes of shoreline change can be natural or human-induced (Li *et al*. 2001). On the coast, the primary natural elements are sea level, waves, currents and tides, however, not all of these agents may be present at any particular location. If sea level rises, the coastline is moved landward, whereas if sea level falls, the shoreline is shifted seaward (Masselink and Hughes, 2003). Wave is a primary force of erosion in the coastal area. The energy in a wave is related to meteorological, topographic and hydrographic factors, such as wind speed and distance over which the winds blow. On shallow continental shelves, tide can be the dominant agent in shaping the morphology. Even in wave dominated environments, tidal processes often are a key subordinate element.

Human activities influencing shoreline change include coastal construction, coastal excavation, and climate alteration (Morton, 2003). There are two general categories of erosion control on sand beaches. The first type is hard stabilization or armoring where structures such as seawalls or jetties are built to help protect development along shorelines (Figure 2.5). However, these structures can be destructive to recreational beaches. Coastal managers often use "soft" alternatives to combat coastal erosion on developed stretches of coastline, such as artificial beach nourishment, snow fences, and dune building (Figure 2.6). Beach nourishment is a process of placing sand on an eroding shore in order to restore and maintain recreational beaches.

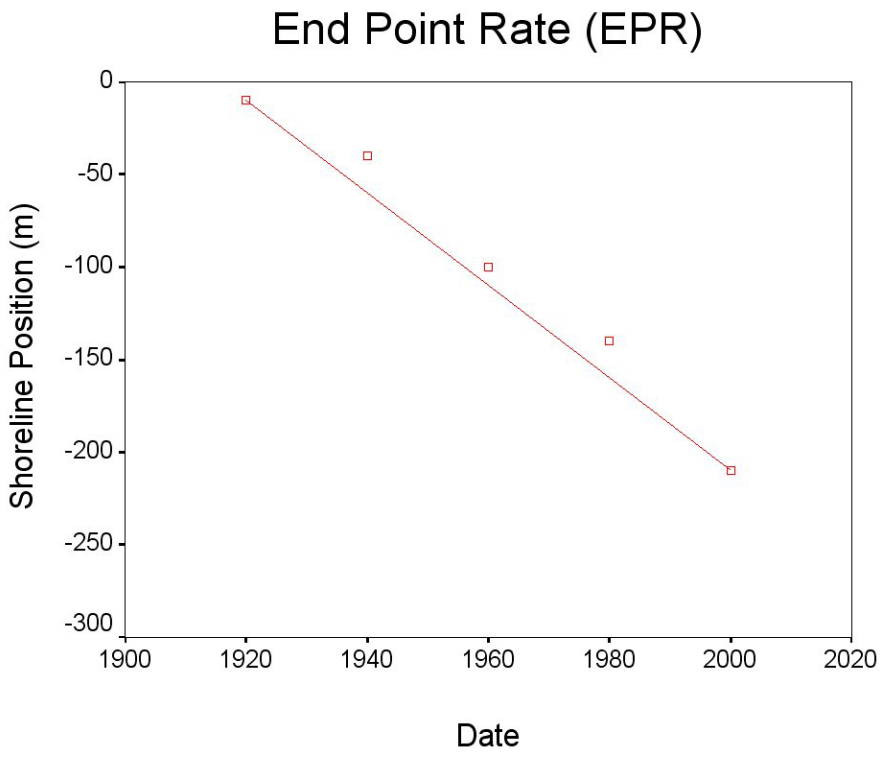

Figure 2.1 Change rate equals slope of the line with EPR (Dolan *et al.* 1991)

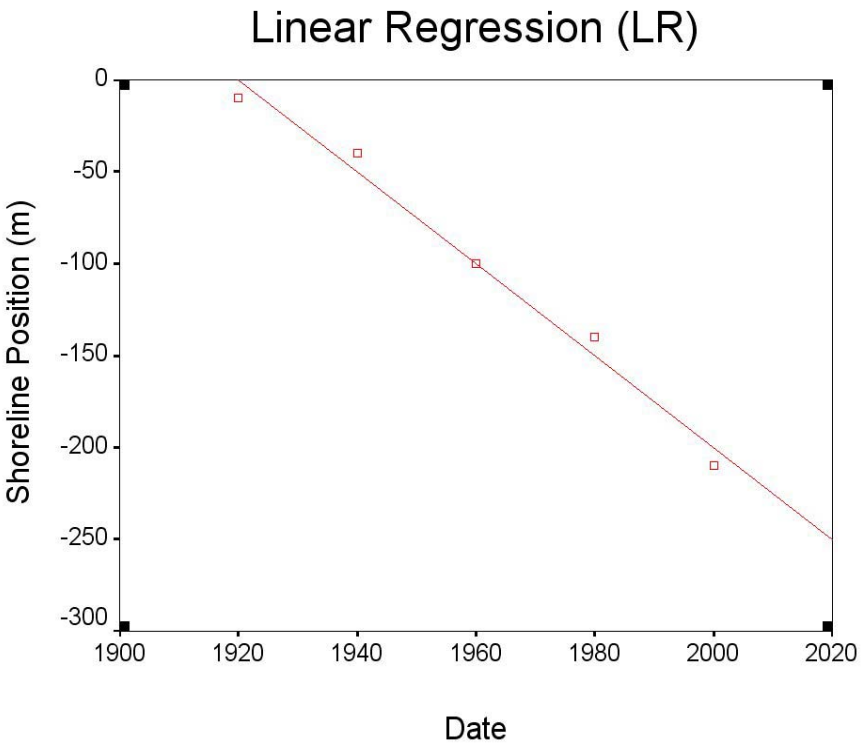

Figure 2.2 Change rate equals slope of the regression line with LR (Dolan *et al.* 1991)

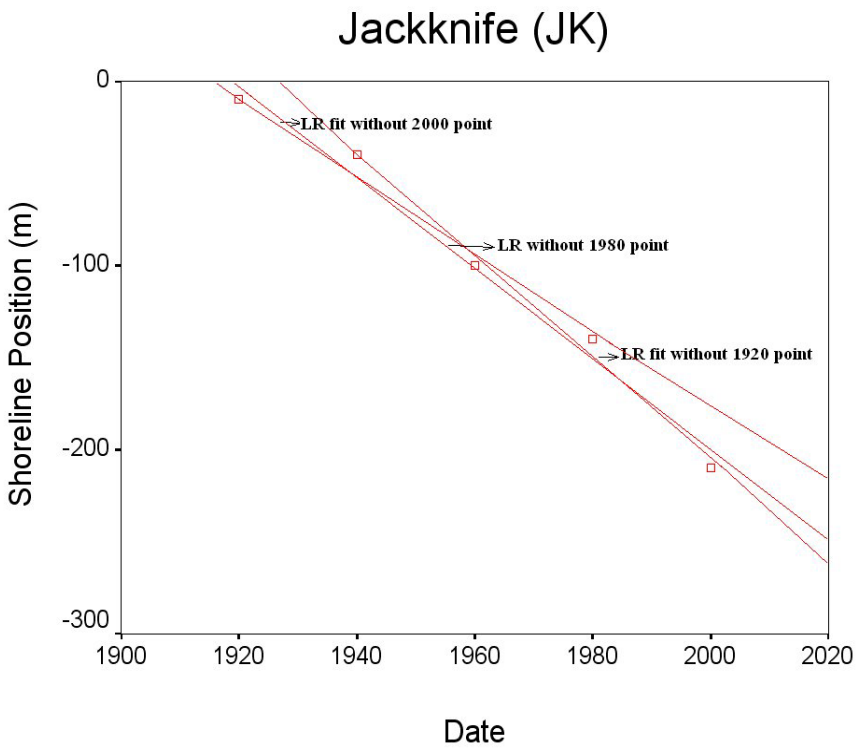

Figure 2.3 Change rate equals averaged slope of the regression lines with JK (Dolan *et al.* 1991)

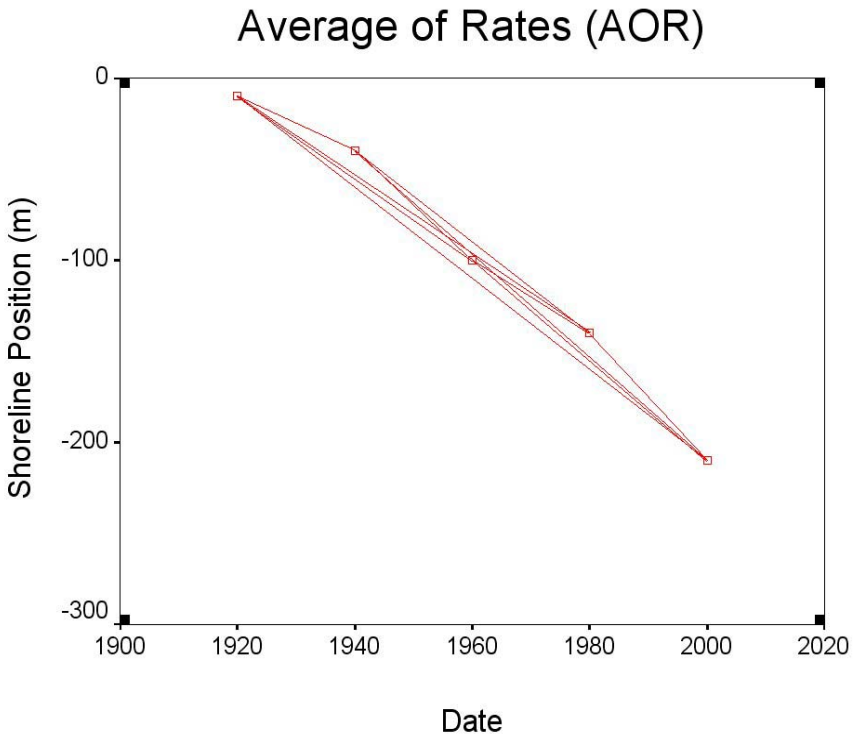

Figure 2.4 Change rate equals averaged slope of the multiple EPR (Dolan *et al.* 1991)

Figure 2.5 Sea wall on Jekyll Island, Georgia

Figure 2.6 Sand dunes on the beach at Jekyll Island, Georgia

CHAPTER 3

STUDY SITES AND DATA SOURCES

The Georgia Bight extends roughly 1,200 km between Cape Hatteras, North Carolina and Cape Canaveral, Florida. The broad, gentle slope of the continental shelf stretches 152 km from the shoreline. Georgia's coastal area is enriched with plentiful marshes, barrier islands, beaches and uplands. It is characterized by 14 relatively short drumstick barrier islands that are separated by large estuaries and backed by expansive salt marshes. Figure 3.1 shows a section of Georgia coast, including Jekyll Island and Sapelo Island. Sapelo Island is the fourth largest of Georgia's barrier islands and most of it remains pristine with minimal development, whereas Jekyll Island is commercially developed. This study only examines the oceanside shoreline changes of the two islands. Though recession or accretion may occur in the back barrier, the change is not undetectable from the aerial photographs. In fact, even the land-water boundary is indiscernible on the photo set because the landward side of Jekyll and Sapelo islands are salt marshes.

3.1 Physical Setting

Geomorphology is the general form of the Earth's surface and the changes that occur to it. The coastal geomorphology of Georgia is of physiographic origin. This Lower Coastal Plain is made up of sediments washed from the Blue Ridge and Piedmont physiographic regions over millions of years. Wave energy on the Georgia coast is low due to the long distance that waves must travel over the continental shelf before reaching the shoreline. Most of the wave energy is dispersed by friction across the bottom of the shelf as waves move toward shore. The principal wave direction responds to the dominant wind direction, which is from the northeast and east. Georgia has semidiurnal tides, namely two high tides and two low tides each day. Tides are the

dominant hydrodynamic agent along the Georgia coast, with a range from 1.8 m to 2.7 m. Spring tidal ranges are 2 m to 3 m, the second highest on the US east coast (Schoettle, 1987). Figure 3.2 shows that the oceanward beach of Jekyll Island is influenced by strong current. The Georgia coast has a moderate subtropical climate, with short winters and long springs and falls. Temperatures range from the 80s to the high 90s during the warmest months of July and August. From December to February, temperatures usually range from the high 40s to the low 70s. Prevailing winds are from the southwest and east in summer and from the north and northeast in winter. Due to its geographic position, the chance of the Georgia shore being hit by a hurricane annually is as low as 5%. Thus, it is rated as one of the safest areas on the Atlantic and Gulf coasts. The Georgia coast experienced five major hurricanes in the 1800s, but has been mostly spared in the 1900s.

Jekyll Island is one of the four commercially developed barrier islands along Georgia's coast. It is located between St. Simons Island to the north and Cumberland Island to the south and is 9.6 km from the Georgia coast (see Figure 3.1). Jekyll Island is 12 km long and 2.4 km wide (Jekyll Island, 2004). It consists of both Pleistocene and Holocene components, which has affected natural communities on the island as well as developmental patterns. The richer, older Pleistocene soils (35,000 years) attracted farming and timbering activities during the plantation period of the island's recent history. The younger Holocene soils (5,000 years old), found at the northern end past Clam Creek and at the southern end, are in the form of dunes and sloughs of a recurved spit. The northernmost point of the island is occupied by oaks and the high tide line cuts into the forest (Figure 3.3). Pine roots appear on the inter-tidal zone. Moving southbound, the shrubby oaks are replaced by an isolated area of low sand dunes thinly covered with grasses and shrubs. To the south of Clam Creek marsh is a freshwater lowland and forest with ponds.

The lower middle regions of the island are marshes and sloughs interspersed with uplands and hammocks. The uplands on south central area of Jekyll Island consist of a series of dune ridges extending toward the southern tip. The lower southern part is an eroded beach with an extensive shrub zone and westward migrating sand dunes. From roughly 1200 m north of the southernmost tip of the island, the eroded bluff beach transitions to an accreting beach with an extensive inter-dune meadow system covered with sea oats and other dune vegetation (Schoettle and Johnson, 1987).

The Jekyll Island Authority operates the Island's facilities in a way that will make it attractive to people of all levels of income. The island boasts about its four championship golf courses, award-winning tennis center, 11-acre summer waves water park, etc. Among the attractions are Clam Creek picnic area, fishing pier and biking trails in the northern part. Mid-island is the Jekyll Island Club National Historic District, a collection of 33 buildings constructed by America's richest families from the late 1800s to early 1900s; the Coastal Encounters Nature Center, Glory Boardwalk and St. Andrews picnic area are located in the southern area (Lenz, 1999).

Sapelo Island is the fourth largest of Georgia's barrier islands at 16 km long and 4.8 km wide, located northeast of Darien (see Figure 3.1). It is separated from Blackbeard Island to the north by Cabretta Inlet, and from Wolf Island to the south by Doboy Sound. Most of the island is composed of Pleistocene soils on the western side and Holocene soils on their eastern sides. Most of Sapelo Island is owned by the State of Georgia, but about 434 acres at the south end still belongs to residents of Hog Hammock (Alkaff, 1997). There is limited utilization of the island and much of the upland is classified as a state wild life management area. The marshes are designated as the Sapelo Island National Research Reserve.

At the northern end of Cabretta on Sapelo Island is an eroded relict Holocene salt marsh exposed in a series of terraces (Figure 3.4). Another feature of this part is the presence of washover fans. This is evidence of beach sand driven landward and formed by the erosion of the dunes. Central Cabretta has a slough behind the beach foredunes that has developed a limited salt mash environment of its own. The southern end of Cabretta and northern end of Nannygoat Beach (Figure 3.5) is occupied by a large number of uprooted trees and exposed old salt marsh muds. The sand dunes vary from poorly-developed to well-developed on Nannygoat Beach. At the southern end, the lines of dunes swing around the tip in great arcs (The University of Georgia Marine Institute, 2001).

3.2 Data Sources

Vertical aerial photographys are extensively used for shoreline change detection. Data used for this research consist of multiple sources, which include DRG's made from hardcopy USGS topographic quadrangles, aerial photographs, DOQQs and lidar images. A DRG is a scanned version of a hardcopy USGS topographic quadrangle. U.S.Geological Survey topographic maps at a scale of 1:24,000 show areas in detail useful for engineering, and local area planning. They are the most widely used maps for coastal studies. The 7.5-minute, 1:24,000-scale quadrangle map sets of 1954/1957 were compiled for coastal Georgia by the U.S. Coast and Geodetic Survey. They are cast on the North American Datum (NAD) of 1927 (NAD27) and a polyconic projection. The DRG is made by scanning a printed map at a minimum of 250 dots per inch (dpi). The raster image is geo-referenced and referenced to the Universal Transverse Mercator (UTM) projection. Colors are standardized to remove scanner limitations and artifacts. The image is compressed to reduce its size. The final result is a compressed TIFF file that ranges from 5 to 15 megabytes in size. The horizontal positional

accuracy of the DRG matches the accuracy of the source map. The 1:24,000-scale DRG at 250 dpi will have a ground sample distance of 2.4 m.

The aerial photographs used for this study were taken by Keystone Aerial Surveys, Inc. on February 23 and 24, 1974, at a flight height of 1828.8 m (6000 ft). These black-and-white 9 in ×9 in vertical aerial photographs are at a scale of 1:12,000. A DOQQ is a scanned and orthorectified aerial photograph in which terrain relief displacements and distortions caused by tilt of the aircraft or camera lens have been eliminated. It combines the image characteristics of a photograph with the geometric qualities of a map. The USGS 3.75-minute DOQQs used in this project are black-and-white images with a 1-meter spatial resolution. They meet NMAS for 1:12,000-scale maps which requires 90% of well-defined test points must fall within 10 m of their real location. The original aerial photographs were taken on January 31, 1993 at a scale of 1:12,000. The DOQQs were cast to the UTM projection and referenced to the NAD83.

Airborne lidar is a new technique to obtain highly accurate and detailed topographic measurements of the Earth's surface. Lidar data used in this research were retrieved from the website of NOAA Coastal Service Center (http://www.csc.noaa.gov/cgi-bin/crs/tcm/ldart_start.pl). The center is located in Charleston, South Carolina. The instrument used for acquisition is called the Airborne Topographic Mapper, which is a scanning lidar developed and used by National Aeronautics and Space Administration for observing the Earth's topography for several scientific applications. The flights mainly take place during the fall, when the beach is generally at its widest. All flights are timed to coincide with low tide when the beach is most exposed, but data should not be considered tidally controlled. This data set was taken on October 11, 1999, with a horizontal accuracy better than 50 cm and a vertical accuracy of 15 cm. The X and Y coordinates were registered to the NAD83, and Z coordinates

were referenced to the North American Vertical Datum of 1988 (NAVD88), which is a best-fit geoid that attempts to match mean sea level (MSL) for as many places as possible. The lidar beach elevation data were displayed in a grid format, in which each cell was assigned a value based on surrounding elevation points. This gives the data an even and continuous distribution, resulting in a smooth surface when displayed.

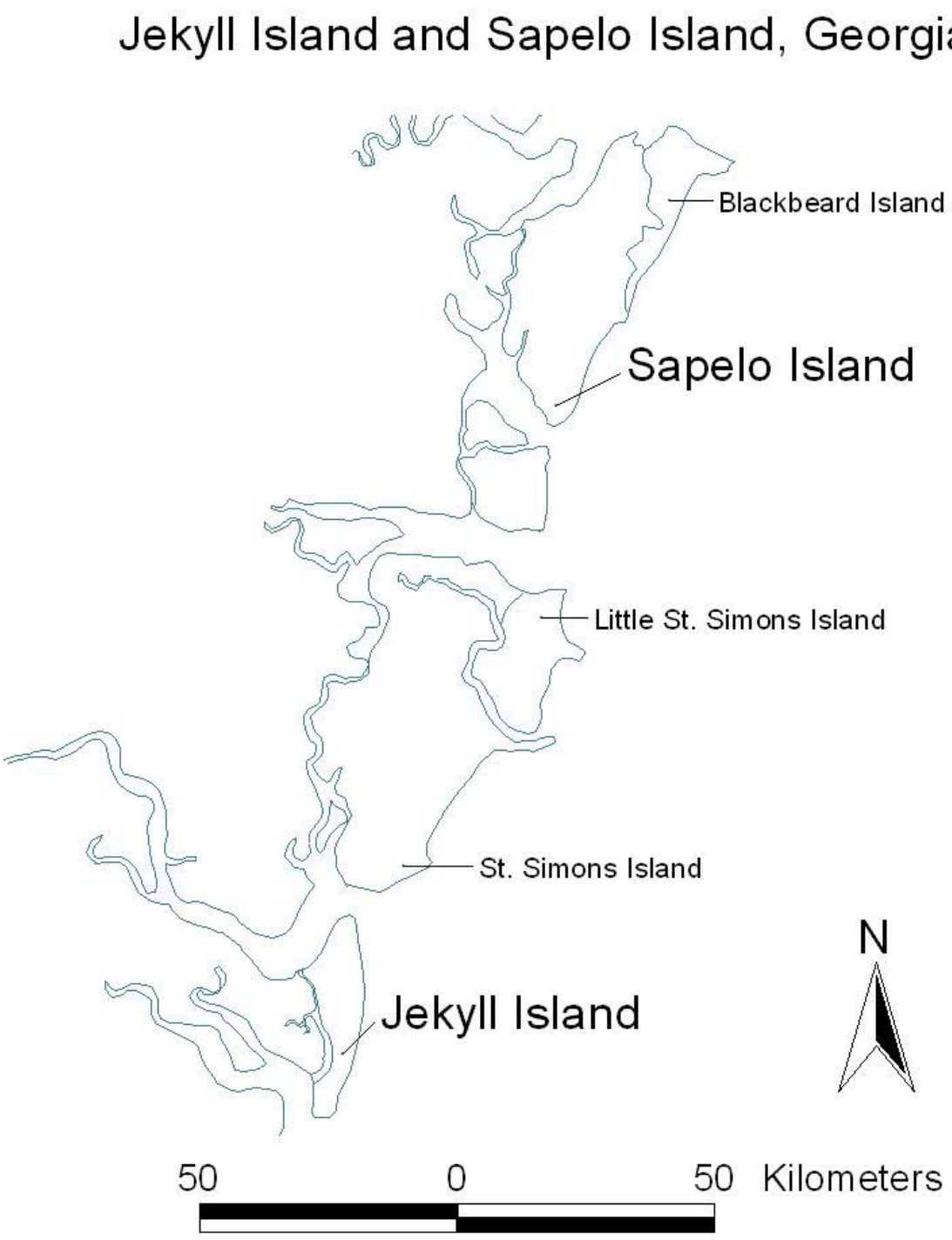

Figure 3.1 Jekyll Island and Sapelo Island, Georgia

Figure 3.2 Sign of current caution on the oceanward beach of Jekyll Island, Georgia

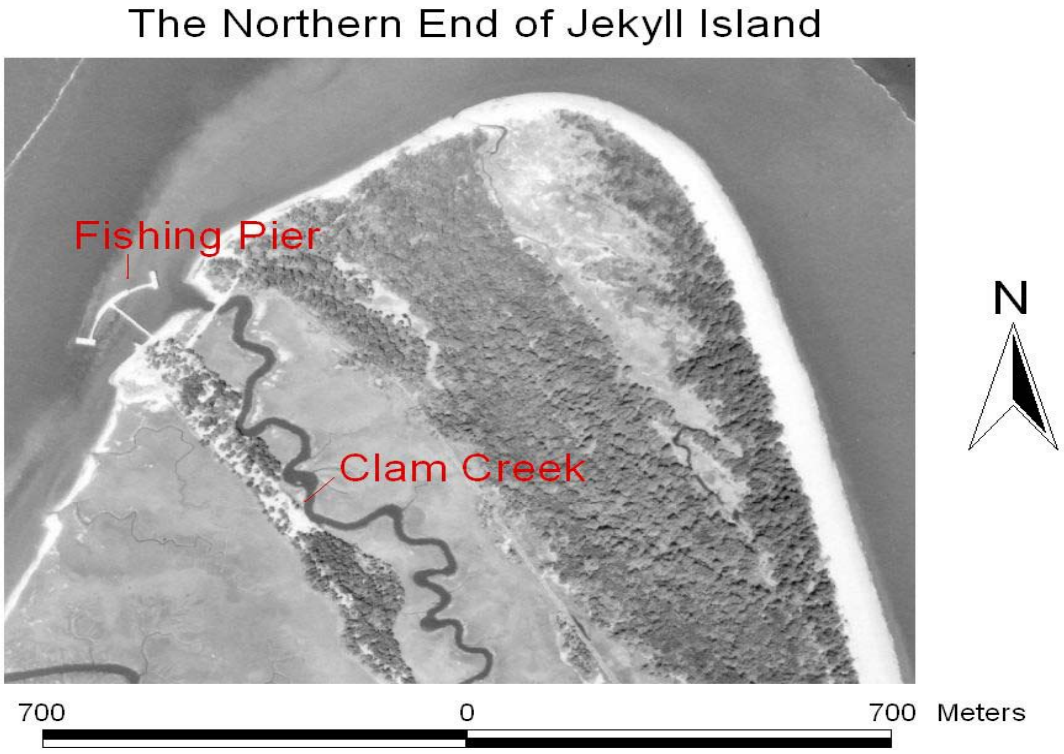

Figure 3.3 Aerial photograph of the northern end of Jekyll Island

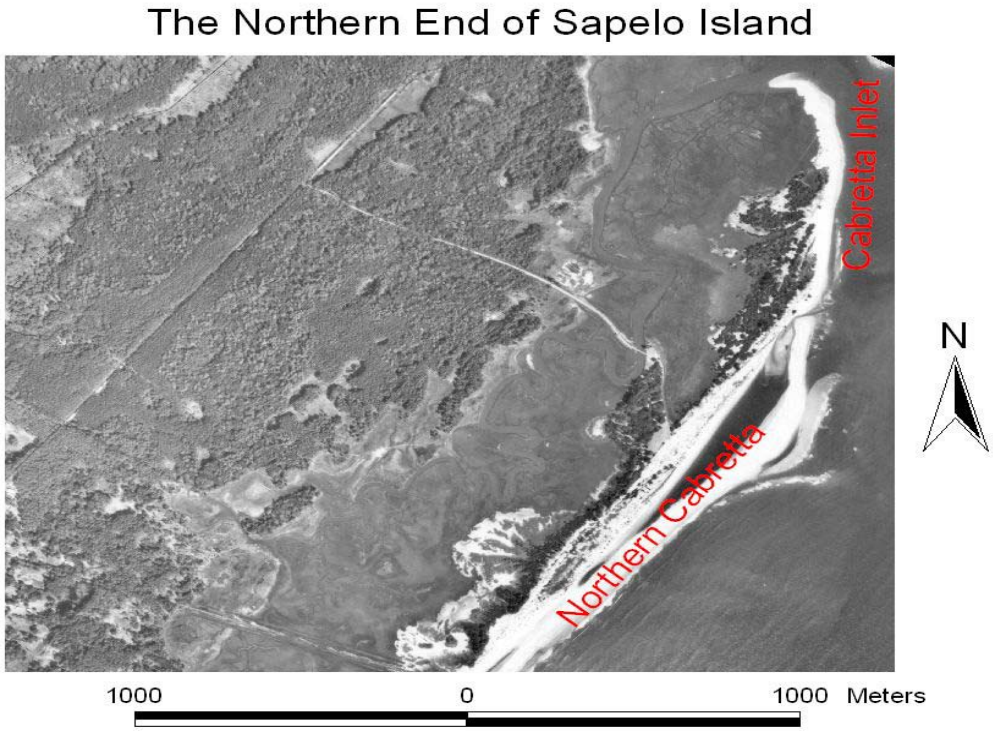

Figure 3.4 Aerial photograph of the northern end of Sapelo Island

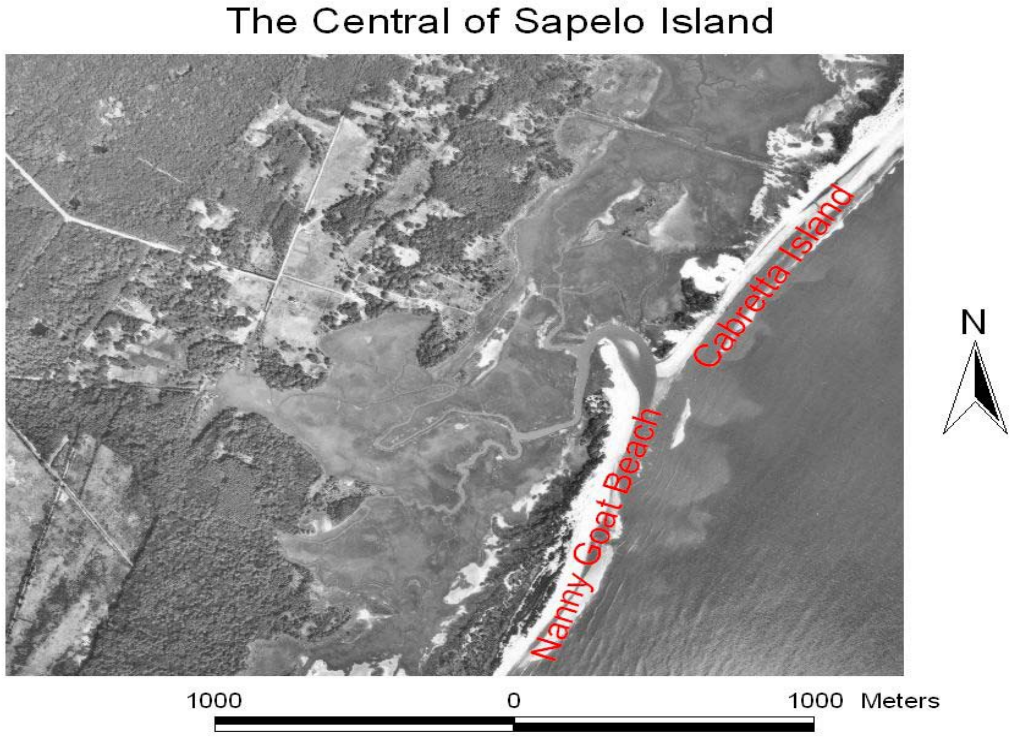

Figure 3.5 Aerial photograph of the central part of Sapelo Island

CHAPTER 4

METHODOLOGY

The conceptual design of the methodology to detect shoreline change is straightforward. In a simplistic sense, this task is completed by tracing the land-water boundary from various resources, overlaying them and then computing rate-of-change. In a realistic sense, this procedure is greatly complicated by environmental and image characteristics. Essentially, change detection requires the ability to use multi-temporal data sets to quantify temporal effects. After considered the cost effect and geometric accuracy of different schemes, GIS strategy was used in this research. The GIS technique simplifies the integration of a variety of data types by allowing conversion to a common projection, datum and coordinate system.

4.1 Map Projection

The 1954 (Sapelo) and 1957 (Jekyll) DRG map sets were obtained in TIFF format from USGS and imported into ERDAS Imagine software, version 8.6. Registering the scanned image to ground coordinates is a plane-to-plane transformation. The four bounding points of the USGS 7.5-minute quadrangle were selected as the control points. First, ground control points (GCPs) were converted from geographical coordinates to a plane system through the process of map projection (parameters are shown in Table 4.1). Ground control points refers to physical points on the ground whose ground positions are known with respect to some horizontal coordinate system or vertical datum (Lillesand and Kiefer, 2000). Second, the UTM coordinates obtained from the map projection process were used as reference coordinates to transform the scanned image to a ground coordinate system. A first order polynomial model was used as the geometric model. A first order transformation can be used to project raw imagery to another planar map

projection and convert a planar map projection to another planar map projection. Last, the resample application was used to transform the scanned file to a coordinate frame of pixels using nearest neighbor resampling method. The critical value for total control point error is set to one pixel in this project.

4.2 Aerial Photograph Rectification

Shorelines from 1974 were mapped using black-and-white vertical aerial photographs at a scale of 1:12,000. Three sections of aerial photographs were mosaicked for the Sapelo shoreline. It took four pieces of aerial photographs to cover the oceanside shoreline of Jekyll islands. Because aerial photographs are distorted and lack a spatial reference, they must be rectified before being brought into a GIS environment. Various algorithms have been used to rectify the data to a scaled, non-tilted condition, such as a least squares adjustment.

The paper aerial photographs were digitally scanned at 250 dpi with a flatbed scanner and imported into ERDAS Imagine software, Version 8.6, for rectification. Rectification of aerial photographs involves the establishment of ground control points that link each photo to its corresponding aerial coverage on a DOQ which served as the reference image.

Ground control points were manually chosen on the aerial photographs that matched points on the DOQQs. The most accurate GCPs are geodetic markers, such as bench marks, for which are ground surveyed but hardly ever visible at photo scale. Secondary GCPs include anthropogenic and natural features that are distinct and common to both data sets, such as road intersections, low-relief building corners and near-shore boulders. Typically, GCPs were evenly distributed throughout each unrectified photograph to correct the distortion errors caused by camera tilt. To minimize the errors related to topographic relief displacement, GCPs were preferentially selected near the shore zone. Selecting GCPs at high-relief locations introduces

significant errors into the rectification process. Where stable control points are difficult to establish, less reliable points, such as river meanders, were used. Six to 12 GCPs were selected for each aerial photograph depending on the availability of suitable control points. Using more GCPs usually improves the accuracy.

Once all the GCPs were established, transformation coefficients were computed using the first order polynomial method. This method corrects all inherent errors and is not specific to tilt or scale variations. The result is a "best fit" position for all control points on an aerial photograph. After a correction factor is computed, coordinates were transformed and resampled to create the rectified image.

4.3 Delineation of Shorelines

A coastline is the line that separates a land surface from an ocean or sea. However, in reality the position of the shoreline is highly variable because of the dynamic nature of the coastal region. Water levels vary due to tides and waves. The first challenge in detecting shoreline position change is to define a consistent shoreline feature. In this research all the shorelines were referenced to the mean lower low water (MLLW) datum after being delineated.

The rectified images were compiled into ArcView GIS software, Version3.3, and manual tracing of shorelines was performed to assure reliability and accuracy. On the USGS DRGs, the shoreline is represented by MHW and ready to be delineated (see Figure 4.1). For aerial photographs and DOQQs the shorelines must first be interpreted and then traced. This line generally can be recognized by a change from dark tone to light tones (see Figure 4.2). Correct interpretation of this line is critical to avoid large inaccuracy. All the shorelines were digitized while viewing the images at a scale of 1:1,000 and the polyline tool in ArcView GIS was used.

The ArcView Spatial Analyst extension was used to convert the lidar image into an ArcView grid. The Z coordinate was referenced to the NAVD88, which means that an elevation value of zero is somewhere near the MSL value. Contour lines were generated starting from elevation zero at a five-meter contour interval using the 'create contour' function (see Figure 4.3). The contour line with a value of zero that approximates the MSL was then manually traced.

4.4 Shoreline Registration

It is necessary to distinguish two tidal data---mean low water (MLW) and MLLW. Mean low water is the average height of the low waters over a 19-year period, whereas MLLW is the average height of the lower low waters over a 19-year period (Bates and Jackson, 1984). The differences in positions of the two shoreline data are insignificant for mapping purposes. Before the distance of total shoreline movement can be measured, all the shorelines were registered to MLLW that was used as the reference tidal datum.

The shoreline is represented by MHW on the USGS DRGs. With the knowledge of mean range of tide, which is the difference in height between mean high water and mean low water, MHW can be easily converted to MLLW. For instance, the MHW was referenced to MLLW by moving 2.13 m oceanward because the mean range of tide of Jekyll Island in 1957 was about 2.13 m (7.0 ft). The MSL extracted from lidar data was referenced to MLLW in the same manner.

The exact flight time of the aerial photograph acquisition and DOQQ are not available, however, the flight specifications require the images be acquired at a high sun angle with minimum shadows. Based on this requirement, it was inferred that the images were obtained between 10:00am and 2:00pm. The Keystone Aerial Surveys, Inc. also confirmed that the flight was flown between 10:00am and 2:00pm. Features had little shadow on the photos and

direction of the shadow indicated that the photo was taken before noontime. Therefore, I assumed that the flights were flown at 11:30 am. The height of high and low water for Jekyll Island and Sapelo Island were obtained from the 1974 and 1993 Tide Tables published by NOAA (see Table 4.2 & 4.3), which were based on MLW and MLLW, respectively. The exact tidal heights at 11:30 am were calculated by using parameters, such as duration of rise or fall and range of tide, provided by the 1974 and 1993 Tide Tables, and then converted to MLLW.

4.5 Shoreline Change Rate Computation

The distance of total shoreline movement was measured by about 250 transects which were constructed perpendicular across shorelines. This distance was divided by the time interval to calculate the change rate that was expressed in terms of distance of change per year. All shorelines were overlain in ArcView GIS software. The Metric Mapping ArcView extension, developed by Keqi Zhang, in the Laboratory for Coastal Research at Florida International University, was used to measure the distance of total shoreline movement between 1954 -1974, 1974 -1993, and 1954 -1999 for Sapelo Island, 1957-1974, 1974 -1993, and 1957-1999 for Jekyll Island First, the polyline tool was used to manually construct a spine just off-shore of the most seaward shoreline to approximate the general trend of shorelines. This spine is an artificial line and provides a start point for the transect lines. Ideally, the spine should be parallel to shorelines so transects will be perpendicular to shorelines, but it is impossible to create such a spine to parallel to all shorelines. Second, a series of transects perpendicular to the baseline were generated with 50 m intervals (see Figure 4.4). The distance from each shoreline to the baseline was measured along transects. Last, EPR was used to calculate average annual rates of change along transects. Positive values represent accretion whereas negative ones indicate recession.

4.6 Shoreline Change Comparison

After the average annual rates of shoreline change were derived, the tables were imported into SPSS, Version 11.0, for statistical analysis. The significance level was chosen to be 5% (P=0.05) for all the statistical analyses conducted in this research. A Mann-Whitney test or two-sample difference of means t Test were conducted on the annual erosion rates, accretion rates and annual mean change rates (regardless of direction) of the study sites to see if the rates of the two islands differed significantly during the same period of time. First, one-sample Kolmogorov-Smirnov test (two-tailed) was conducted on the nine data sets---three data sets from each category--- to test their normality. If data were normally distributed, a two-sample difference of means t Test (two-tailed) was applied to compare annual erosion rates, accretion rates and mean shoreline change rates. Otherwise, the Mann-Whitney test was conducted.

Differences in shoreline change patterns of these two barrier islands result from a number of factors. The physical settings of these two islands and human activities took place on them were briefly investigated and compared in this research.

Table 4.1 Parameters of input projection and output projection

	Input Projection	**Output Projection**
Projection Type	Geographic	UTM
Spheroid	Clarke 1866	GRS 1980
Datum	NAD27	NAD83

Table 4.2 1974 tide tables for Jekyll Island and Sapelo Island

	Jekyll				Sapelo			
Time	5:41	11:34	18:01	0:06	3:17	9:08	15:36	21:23
Height (ft)	0	5.9	-0.2	6.7	-0.5	6.6	-0.5	6.9

Table 4.3 1993 tide tables for Jekyll Island and Sapelo Island

	Jekyll				Sapelo			
Time	1:04	7:52	13:27	20:17	4:35	11:15	17:07	23:28
Height (ft)	7.4	2.2	6.6	1.6	8.0	1.4	7.1	0.6

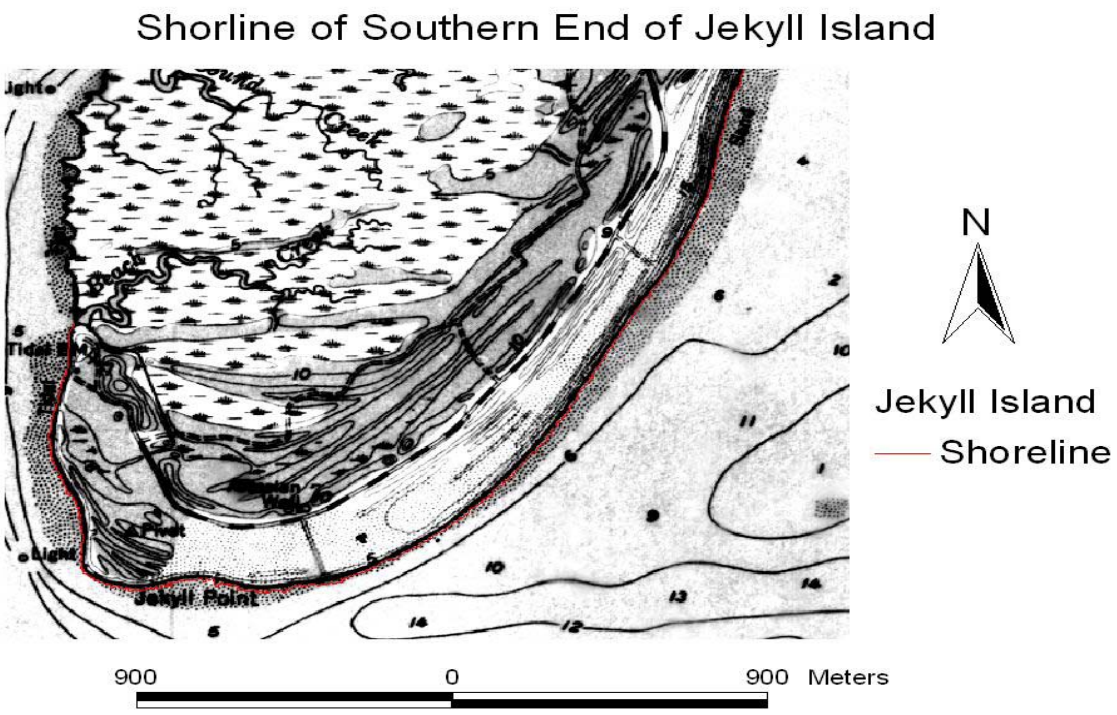

Figure 4.1 Shoreline delineation of southern Jekyll Island on USGS DRG

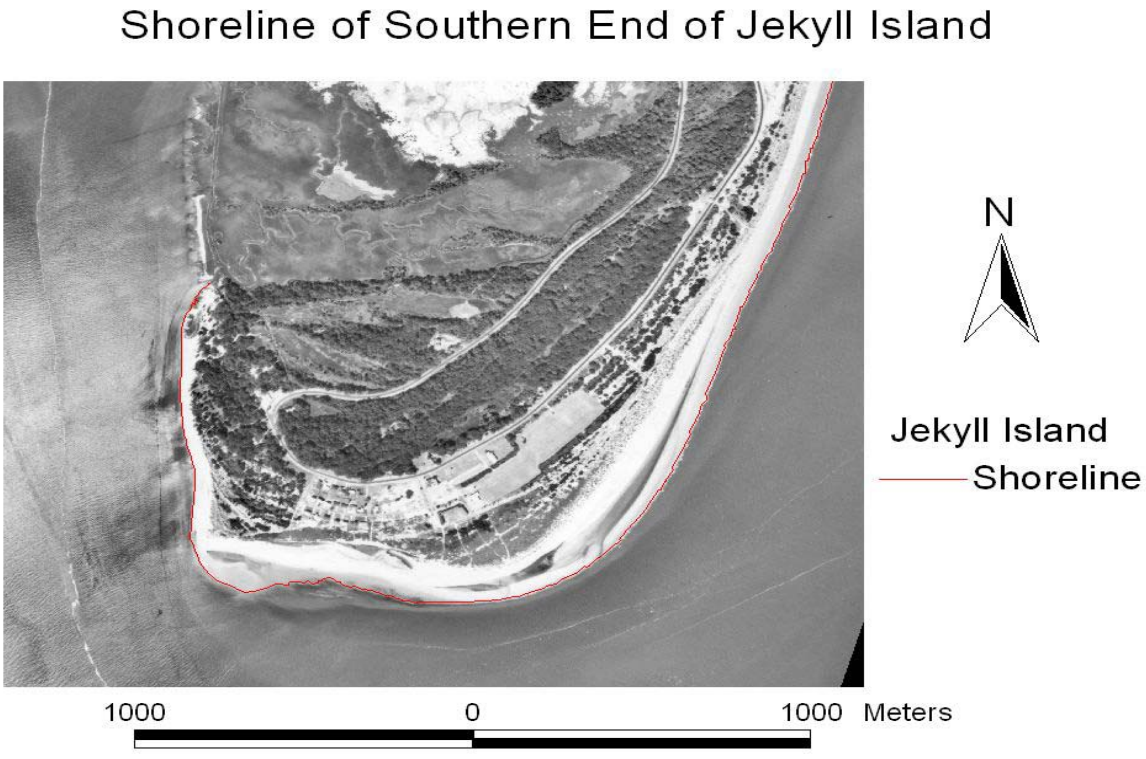

Figure 4.2 Shoreline delineation of southern Jekyll Island on aerial photograph

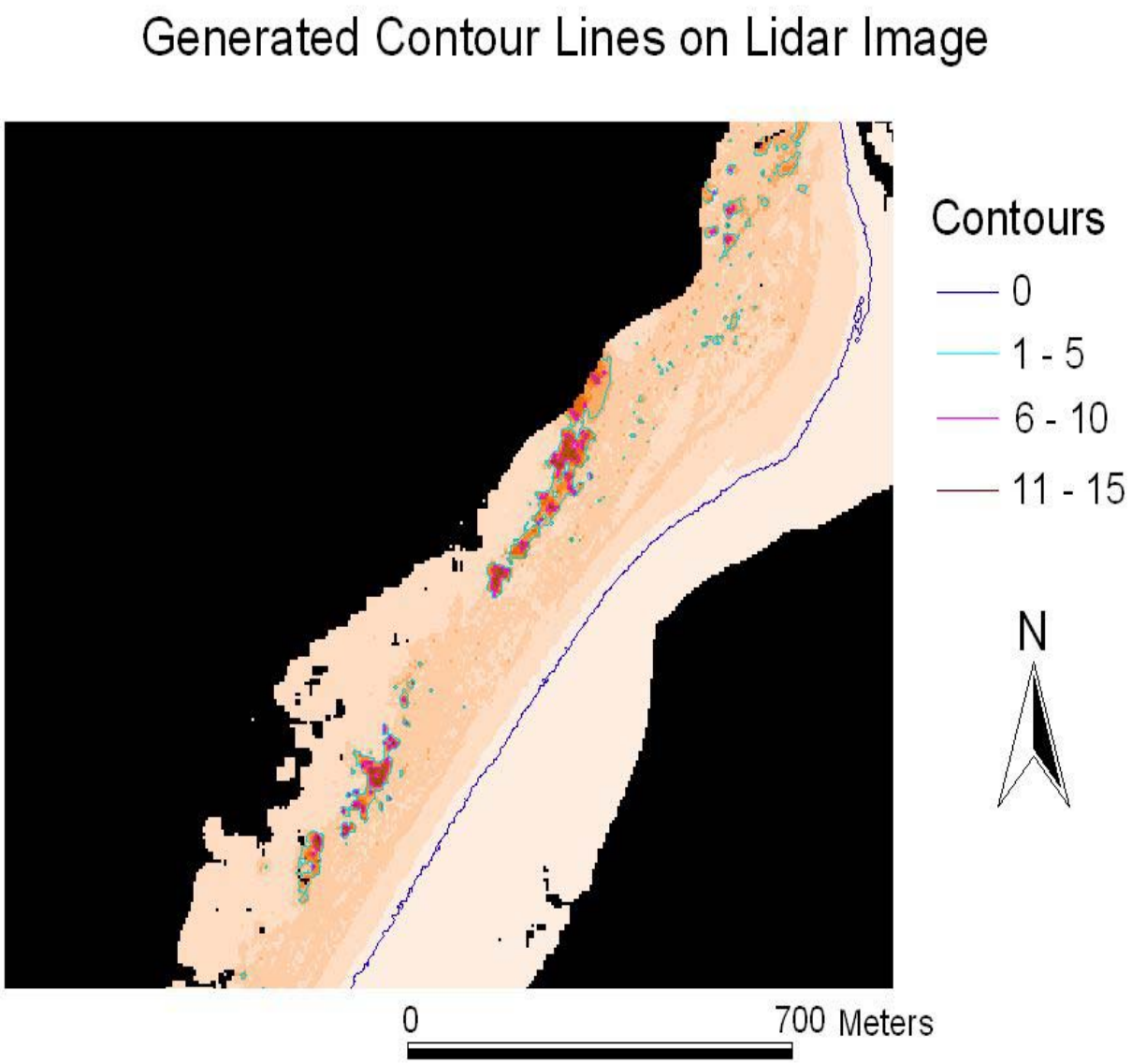

Figure 4.3 Shoreline extraction from the 1999 lidar image

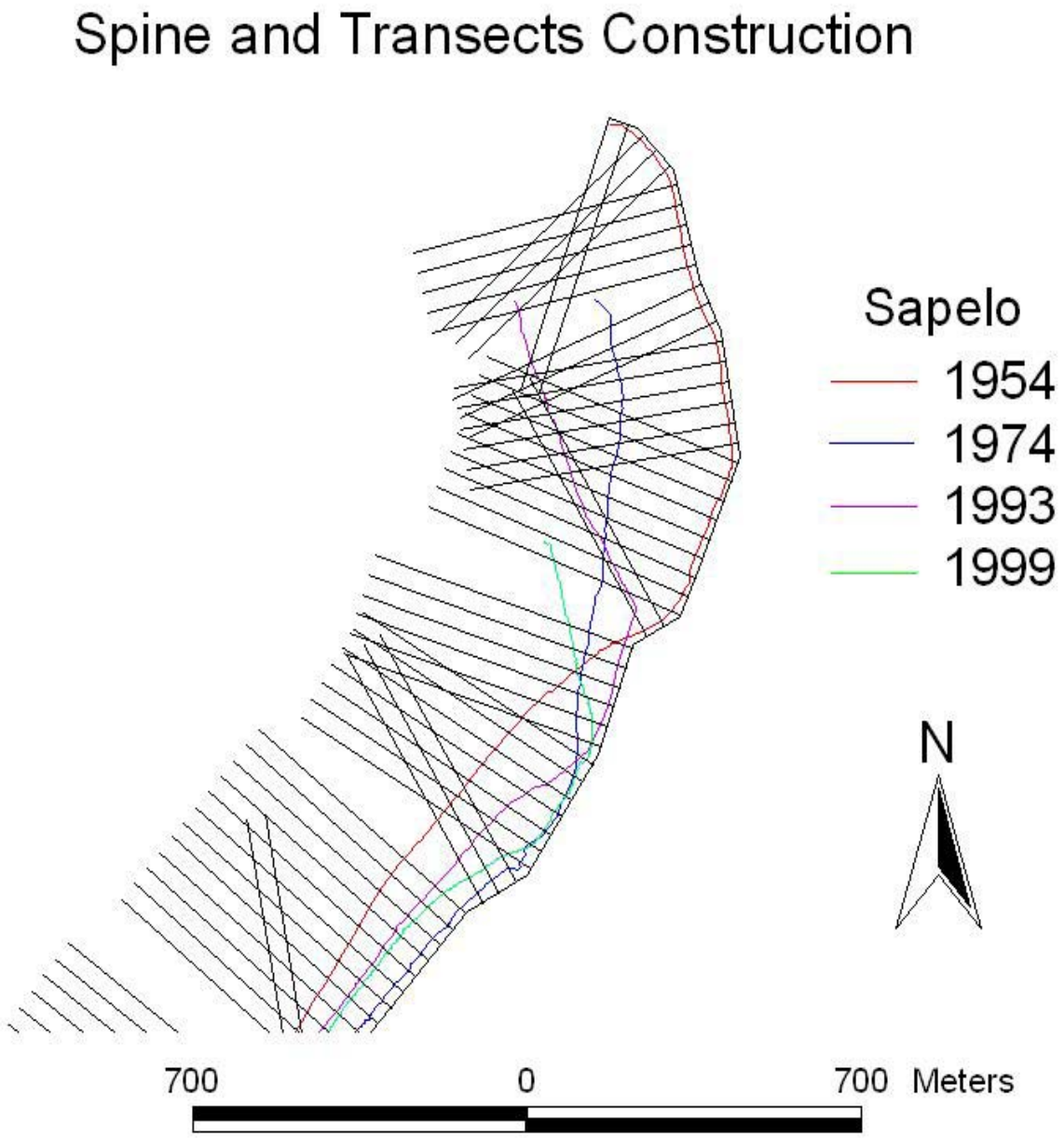

Figure 4.4 An example showing spine and transects construction

CHAPTER 5

RESULTS

5.1 Map Projection

To ensure accuracy of the results, critical values are set for the map re-projection and aerial photograph rectification. Jekyll Island is on one 7.5-min USGS DRG, and Sapelo Island is on two DRGs, namely Cabretta Inlet and Doboy Sound. The total control point errors of each map are listed in Table 5.1. They are below the critical value, one pixel, which corresponds to about 2.4 m on the ground.

5.2 Aerial Photograph Rectification

The total control point errors of each photo summarized in Table 5.2 are smaller than the critical value (one pixel) that equals to about 2.0 m. When all the images were pieced together, the maximum misalignment between two adjacent aerial photographs was four meters on the ground.

5.3 Shoreline Registration

Shorelines traced on the 1950s DRGs were referenced to MLLW by moving 2.13 m and 2.16 m oceanward, as the mean tidal ranges of Jekyll Island in 1957 and Sapelo Island in 1954 are 7.0 ft (2.13 m) and 7.1 ft (2.16 m), respectively. For the 1999 lidar data set, the MSL is 4.21 ft (1.28 m) above MLLW at St. Simons station, which is the closest station to Jekyll Island and Sapelo Island. The MSL was moved 1.28 m oceanward. Shorelines of Jekyll Island and Sapelo Island delineated from the 1974 aerial photograph sets were moved 1.80 m and 1.37 m oceanward based on the computed tidal heights. In the same way, 1993 shorelines of Jekyll and Sapelo islands were moved 1.62 m and 0.42 m, respectively (Table 5.3).

5.4 Shoreline Change Rate Computation

The rate calculation results are listed in Table 5.4 and are shown graphically in Figure 5.1 and Figure 5.2 with negative values representing recession and positive values indicating accretion. The rates from the three selected time intervals are similar and complementary for both islands.

5.5 Shoreline Change Comparison

What statistical test to conduct for comparing the means of two samples depends on the normality of the sample data. For Sapelo Island only 1974-1993 and 1954-1999 accretion data were not from normally distributed populations, whereas 1957-1974 erosion data were the only normally distributed population for Jekyll Island. The one-sample Kolmogorov-Smirnov test results are summarized in Table 5.5.

The two-sample difference of means t Test (two-tailed) was applied to the 1954-1974 (1957-1974) erosion data sets, whereas Mann-Whitney test (two-tailed) was conducted with all other data sets. The mean erosion rates, accretion rates and annual change rates were statistically different during 1954-1974 (1957-1974) and 1974-1993 for the two islands. The average accretion rates and annual change rates differed significantly during 1954-1999 (1957-1999), while the mean recession rates were not statistically different (Table 5.6). Because these two barrier islands are within the same hydrodynamic regime and in a similar physical setting, the significant differences in the mean erosion rates, accretion rates and annual change rates are assumed to result from the impacts of human activities.

However, both islands exhibited a pattern of north-to-south sediment transport as the northern ends of the study areas were receding and the southern ends were advancing. This pattern is shown clearly from Figure 5.3, 5.4, 5.5 and 5.6.

Table 5.1 Accuracy for map projection of Jekyll and Sapelo islands

Jekyll	**Control point Error (cm)**			X 0.0069	Y 0.0073	**Total 0.0101**	
Point#	**X input**	**Y input**	**X reference**	**Y reference**	**X residual**	**Y residual**	**RMS**
1	3.254	25.289	452346.093	3443588.250	-0.007	0.007	0.010
2	22.116	25.378	464264.323	3443541.372	0.007	-0.007	0.010
3	22.225	3.486	464217.727	3429688.211	-0.007	0.007	0.010
4	3.310	3.426	452283.930	3429734.991	0.007	-0.007	0.010
Cabretta				X 0.0054	Y 0.0117	**Total 0.0129**	
1	1.902	25.055	476276.318	3485068.301	-0.005	0.012	0.013
2	20.687	25.164	488146.988	3485048.374	0.005	-0.012	0.013
3	20.788	3.318	488131.403	3471194.674	-0.005	0.012	0.013
4	1.956	3.255	476244.911	3471214.664	0.005	-0.012	0.013
Doboy				X 0.0078	Y 0.0071	**Total 0.0105**	
1	2.117	25.133	464405.191	3485102.049	-0.008	0.007	0.011
2	20.938	25.005	476276.318	3485068.301	0.008	-0.007	0.011
3	20.775	3.132	476244.911	3471214.664	-0.008	0.007	0.011
4	1.898	3.288	464358.056	3471248.290	0.008	-0.007	0.011

Table 5.2 Accuracy for airphoto rectification of Jekyll and Sapelo islands

Control Point Error (cm)		**X**	**Y**	**Total**
	7-40	0.0085	0.0061	0.0105
	7-41	0.0078	0.0073	0.0107
Jekyll	7-43	0.0082	0.0118	0.0143
	7-101	0.0039	0.0041	0.0056
	4-63	0.0073	0.0074	0.0104
Sapelo	4-64	0.0088	0.0101	0.0134
	4-66	0.0081	0.0022	0.0084

Table 5.3 Computed tidal heights for Jekyll Island and Sapelo Island at 11:30 am

	Jekyll		Sapelo	
Year	1974	1993	1974	1993
Height (cm)	180	162	137	42

Table 5.4 Maximum and mean erosion/accretion rates, mean annual change rates of Jekyll (J) and Sapelo (S) islands during the study periods

Time Periods	1954-1974		1974-1993		1954-1999	
	J	S	J	S	J	S
Rate (m/yr)						
Max Erosion	2	18	3	13	2	7
Max Accretion	21	28	30	21	16	14
Mean Erosion	1	7	1	4	1	1
Mean Accretion	3	6	3	5	3	3
Mean Annual Change	3	6	2	5	2	3

Table 5.5 One-Sample Kolmogorov-Smirnov test results for Jekyll and Sapelo islands

		Erosion		Accretion	
		Sample Size	Significance	Sample Size	Significance
	57-74	39	0.442	275	0.000
J	74-93	184	0.004	134	0.000
	57-99	107	0.012	174	0.000
	54-74	78	0.110	138	0.097
S	74-93	82	0.076	139	0.000
	54-99	48	0.054	143	0.000

Table 5.6 Comparison of average erosion rate, accretion rate and annual change rate of Jekyll Island and Sapelo Island

	Significance		
	Erosion	Accretion	Annual Change
54-74 / 57-74	0.000	0.000	0.000
74-93 / 74-93	0.026	0.000	0.000
54-99 / 57-99	0.906	0.032	0.004

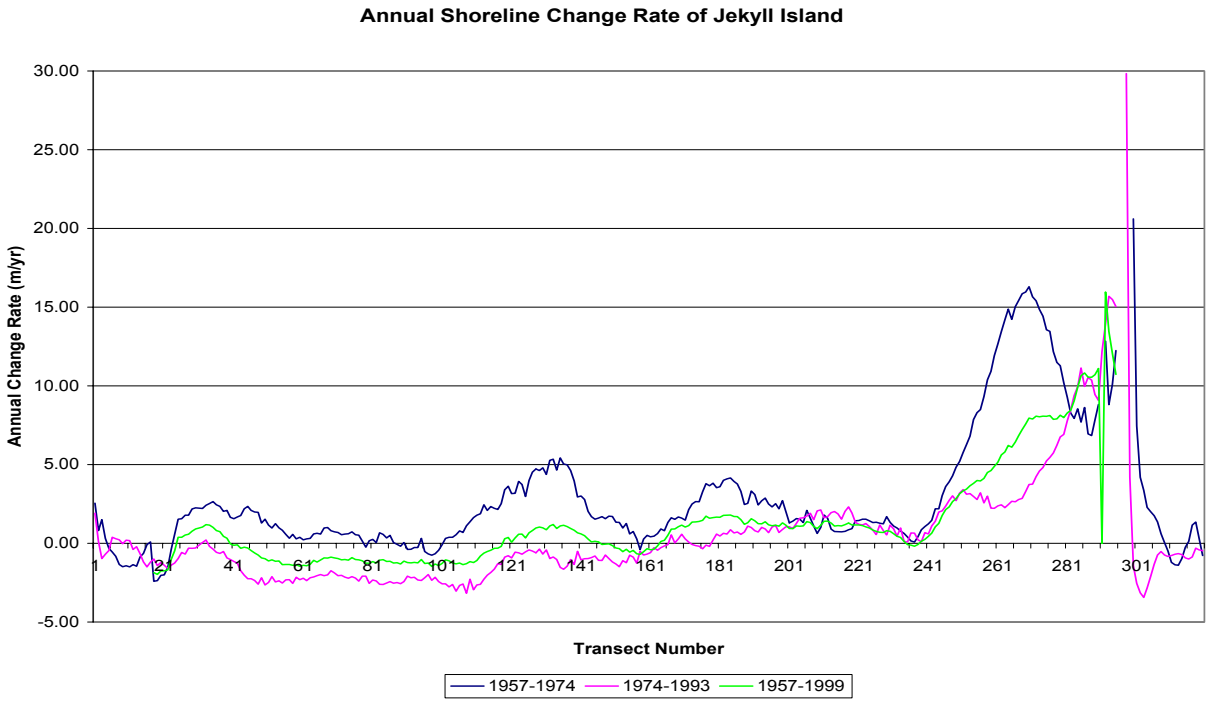

Figure 5.1 Annual shoreline change rates of Jekyll Island during the study periods

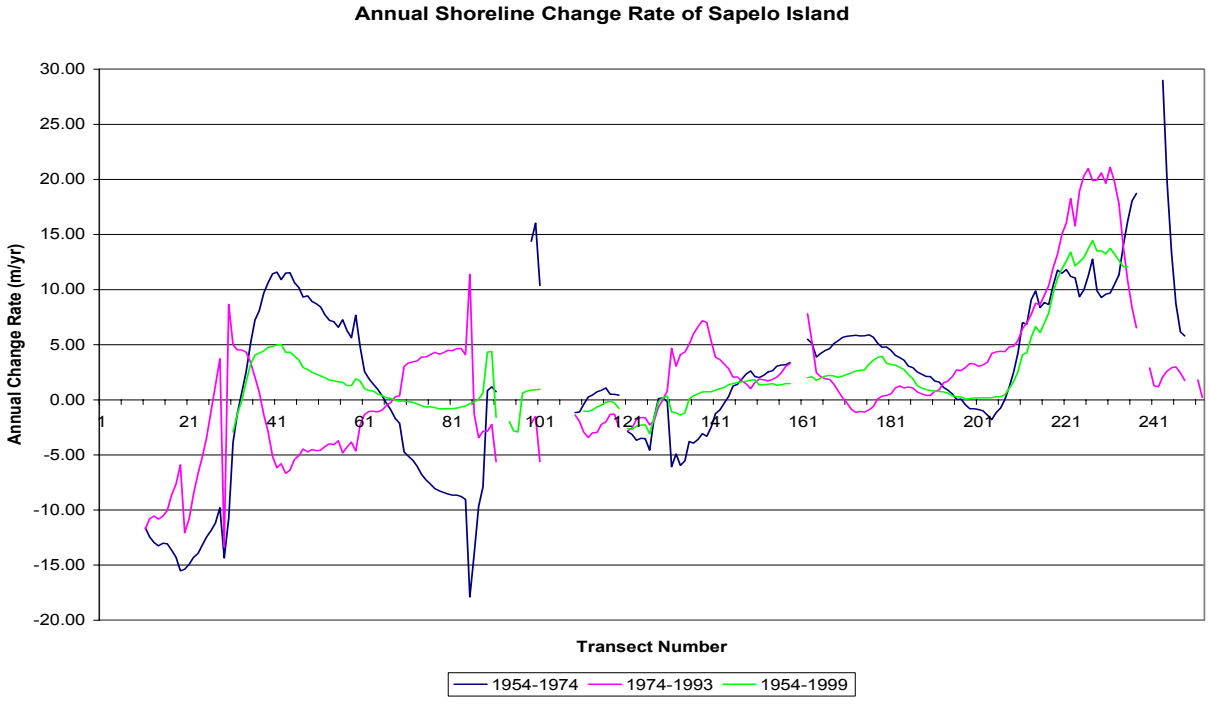

Figure 5.2 Annual shoreline change rates of Sapelo Island during the study periods

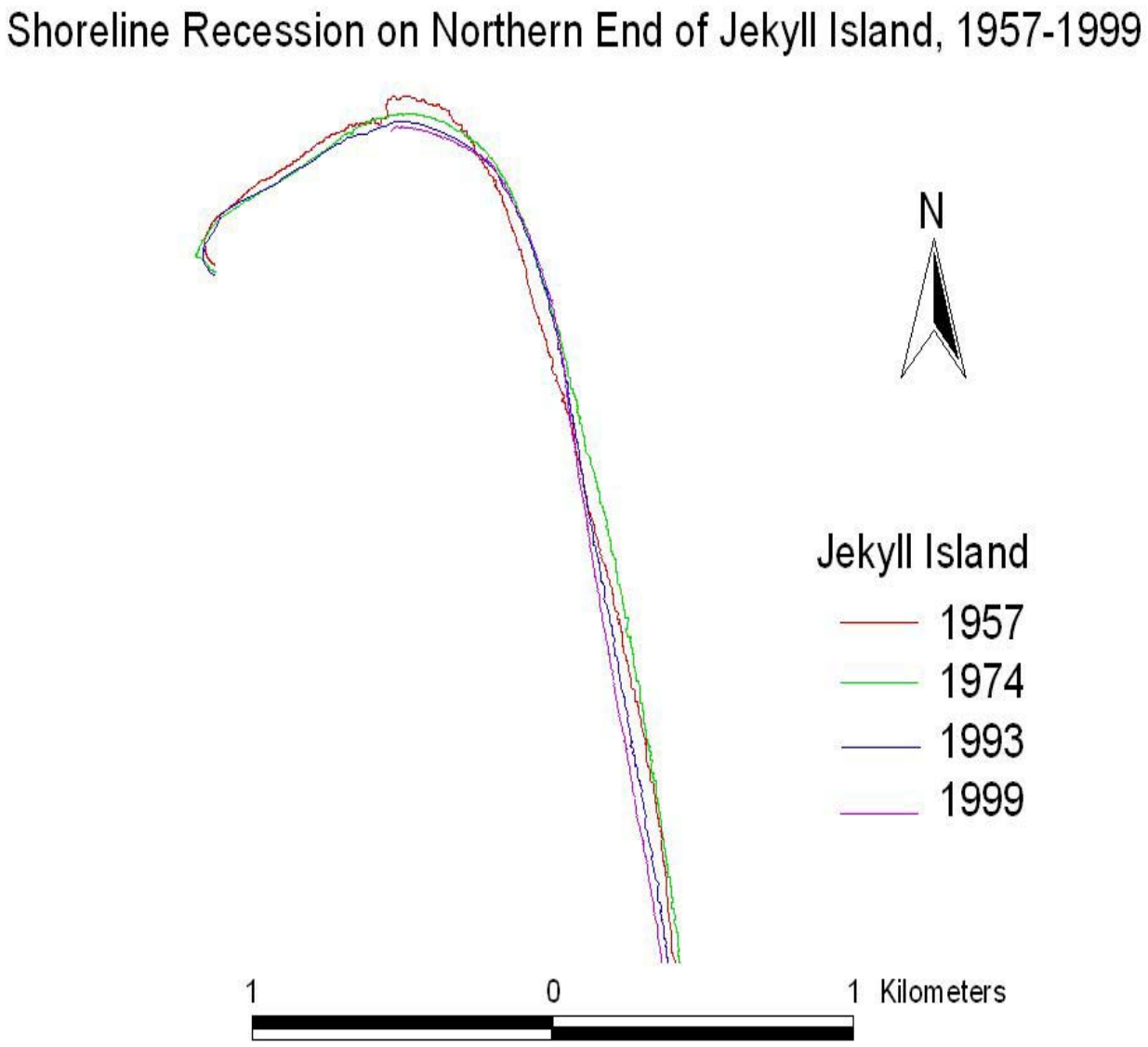

Figure 5.3 Retreat of shoreline on northern end of Jekyll Island, 1957-1999

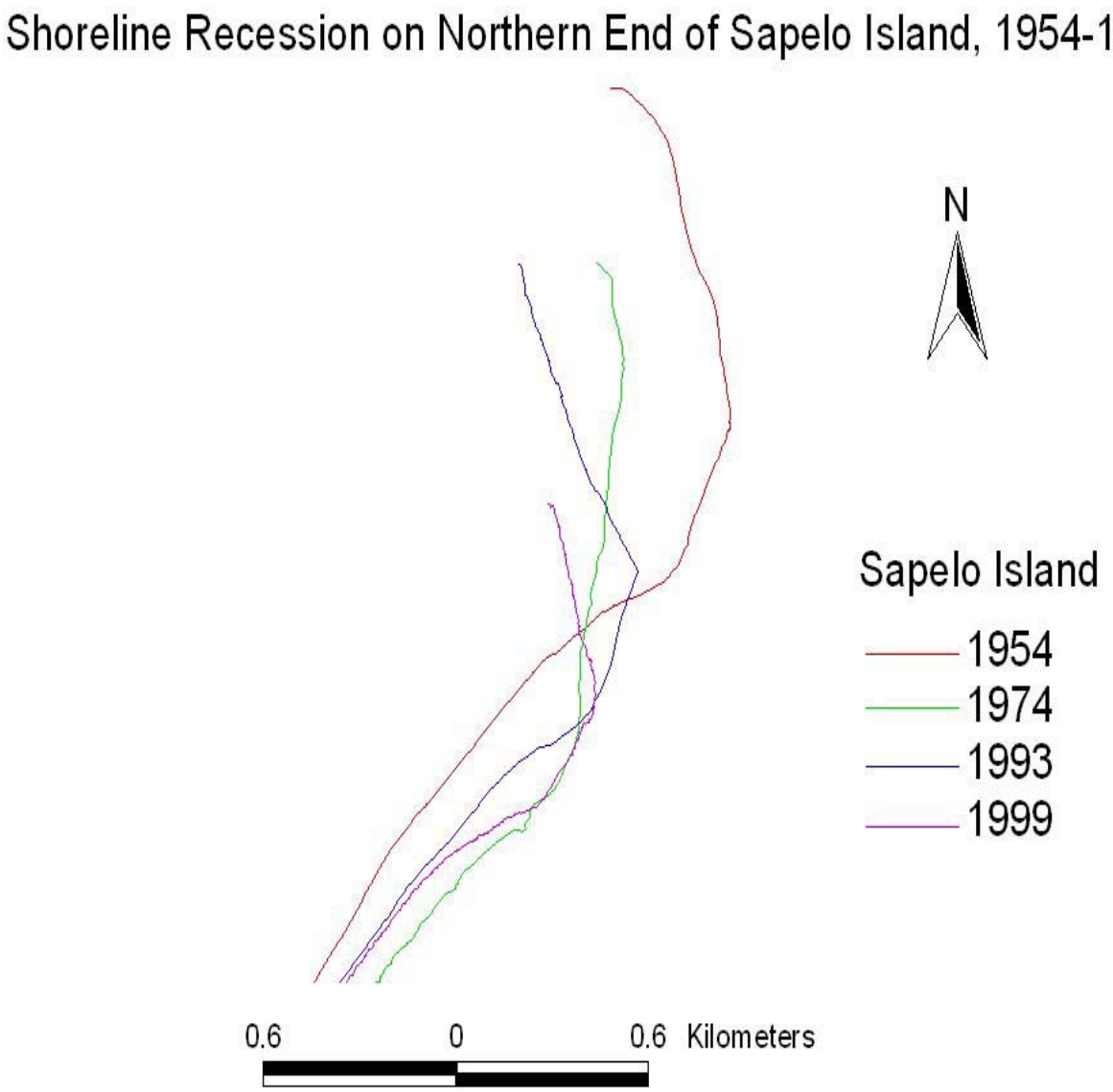

Figure 5.4 Retreat of shoreline on northern end of Sapelo Island, 1954-1999

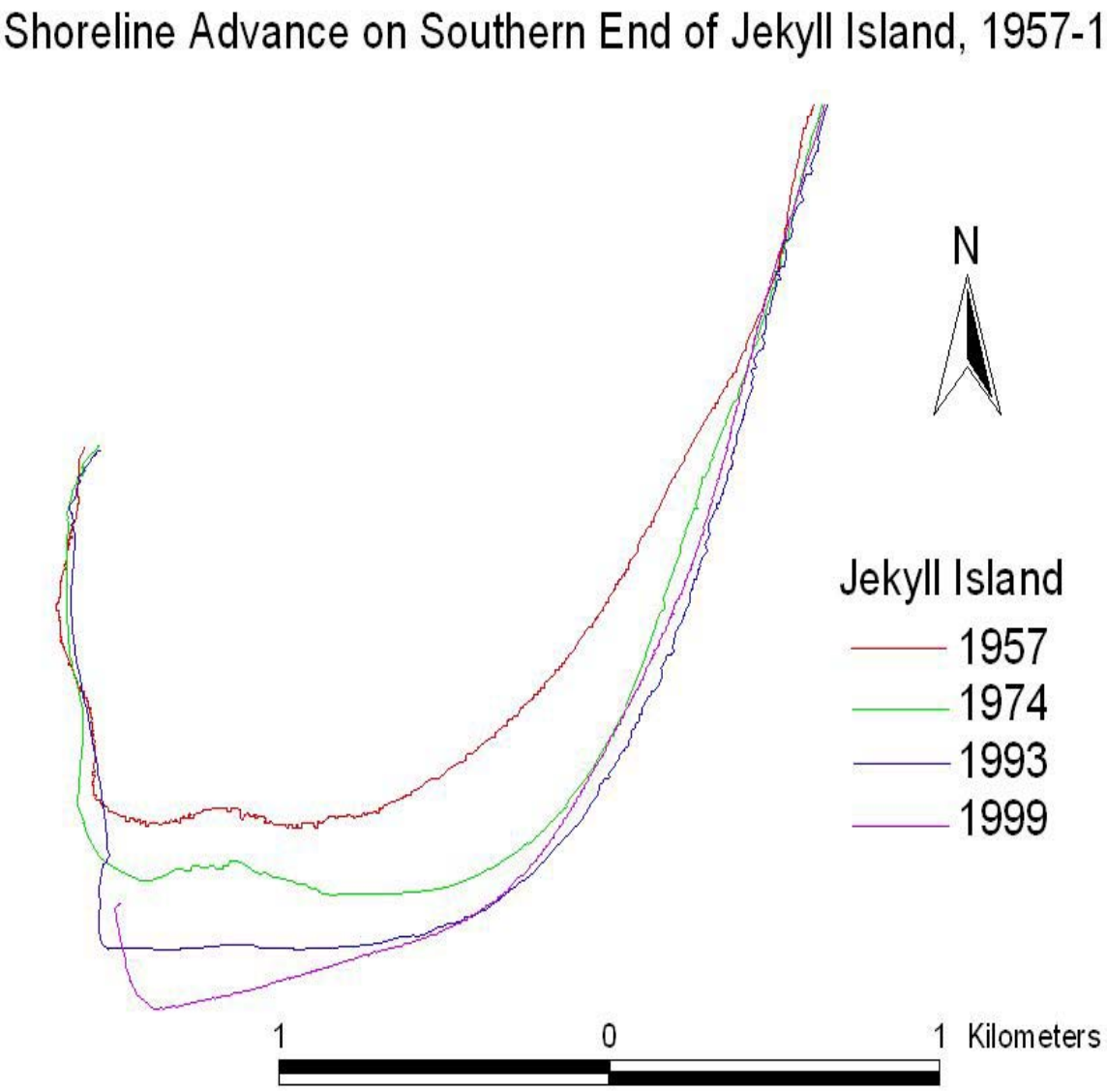

Figure 5.5 Accreting of shoreline on southern end of Jekyll Island, 1957-1999

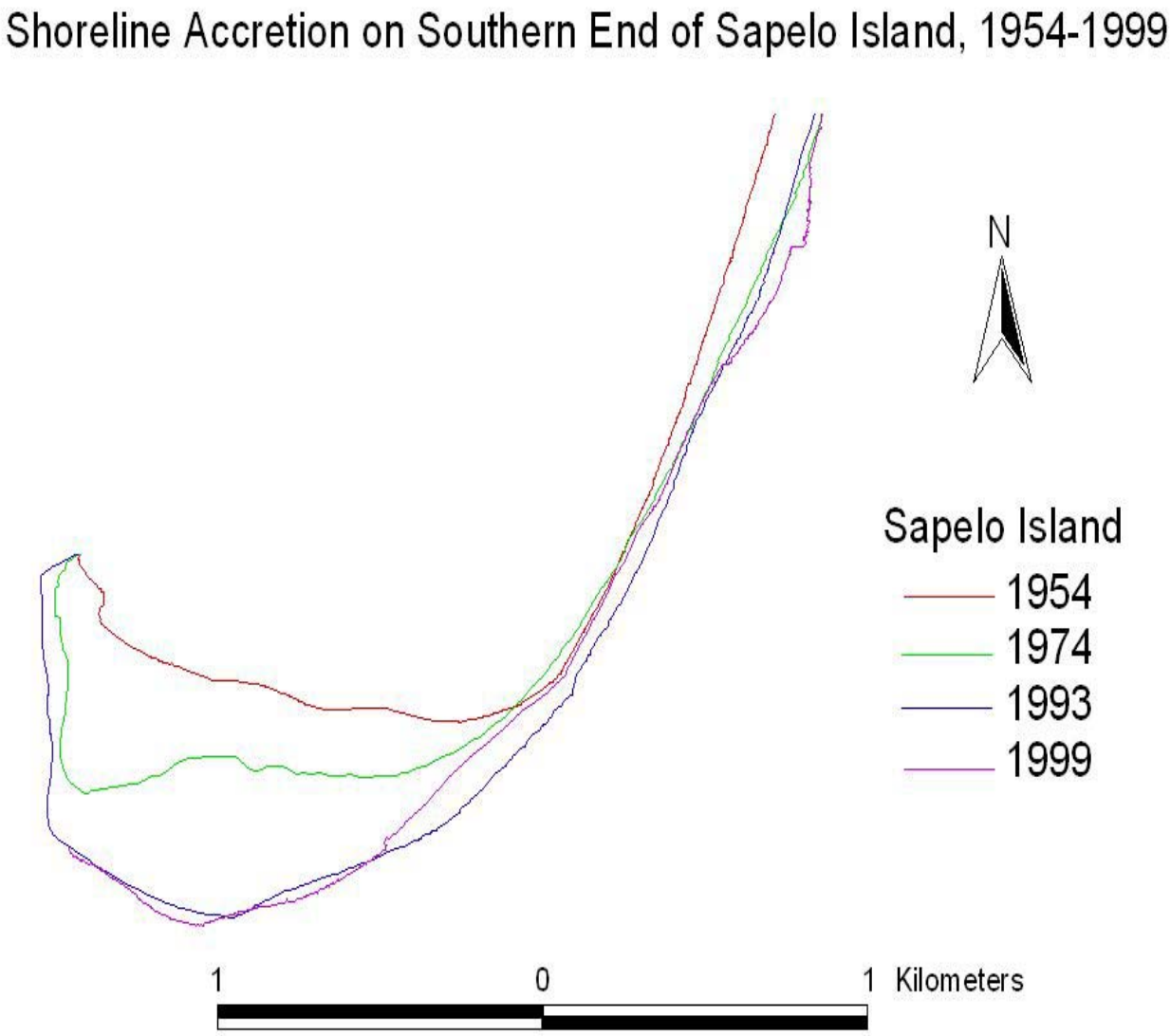

Figure 5.6 Accretion of shoreline on southern end of Sapelo Island, 1954-1999

CHAPTER 6

DISCUSSION AND CONCLUSION

The natural disposition of beach is to change shape constantly and to retreat or advance. Such change is caused by the forces that move the sand, like wind, waves, and tidal currents and by the supply of sand. Georgia barrier islands that are located far from the continental shelf have strong tides and low wave energy. This causes these islands to be shorter and thicker, averaging 8 km in length, which contrasts with the 38 km average length of islands in North Carolina and Florida (Brown, 1977).

Large reservoirs of sand in the form of shoals are seen at the mouths of the inlets at the northern ends of Jekyll and Sapelo islands, resulting from complex interactions between tidal and alongshore currents (Schoettle, 1987). Waves refracting around these inlet shoals create clockwise eddy currents that hold sand close to the north-end beaches. Through southerly-directed alongshore currents and wave refraction, the shoals tend to drift downward and inward toward the upper parts of the islands south of the inlets. The frequent incorporation of inlet shoals to the north gives the islands their drumstick shape.

The southern tips of Jekyll Island and Sapelo Island are recurved. The currents carry sand, which is deposited in shallow areas near barrier islands as shoals and spits. Spits continue to grow in a southerly direction as the alongshore currents continue to deposit sand. The free end of a spit tends to curve inward toward the back of the island. Obliquely approaching waves tend to turn toward the beach and around the tip of the spit, depositing the sand inward and upward, creating the recurved shape.

As indicated previously in Figure 5.1 and Figure 5.2, the seaward beaches (excluding northern and southern tips) of these two islands do not show a consistent retreating or advancing movement, instead they exhibit patterns of irregular receding and accreting. This is because the eastern shorelines are affected mainly by alongshore currents, which cause erosion as well as accretion. The transects of Jekyll Island show a continuous pattern whereas Sapelo Island exhibits a spatially discontinuous pattern. As the Big Hole Creek divides Sapelo Island into Cabretta Island and Nanny Goat Beach, transects are not available in that area. The diagrams also show that the general trend in coastline change for Jekyll Island is more consistent than that of Sapelo during the study periods. Two factors contribute to this phenomenon. The beach on Sapelo Island is in a natural state without any coastal engineering. Conversely, erosion control measures were implemented on Jekyll Island to stabilize the shoreline. In addition, the Big Hole inlet is located in the middle section of Sapelo Island and inlet-adjacent shorelines tend to be unstable due to fluctuations or migrations of inlet position.

Both barrier islands were retreating at the northern ends and advancing at the southern ends due to the north-to-south littoral currents, as shown in Figure 5.3, 5.4, 5.5 and 5.6. Littoral transport is the movement of material by waves and currents on the coastline. The material being transported is mainly sand and gravel, with a small percentage of silt-sized particles and rocks. The Georgia shore is greatly affected by alongshore currents close to barrier islands. Over long time periods and smaller spatial scales, sediment transport along the Georgia coast is primarily southward in corresponding to the dominant wave direction from the northeast. The sediment from the erosion is transported southward and deposited at the south ends of these two barrier islands where dunes are increasing in size. Thus, the islands shift southward. On Sapelo Island, the northern end of Nanny Goat Beach and the southern end of Cabretta is an area of

erosion. The large retreat of the shoreline can be seen by the large number of uprooted trees and the exposure of old salt marsh muds.

The north end beach of Jekyll Island shows remarkable evidence of erosion, with the high tide line reaching into the forest, and the exposed roots of dead oaks and pines (see Figure 6.1). About three square kilometers of beach was lost between 1935 and 1962, with some areas losing nearly 2.4 m of beach a year (Nash, 1977). The outcome from this study matched with previous research result, as the mean erosion rate and maximum erosion rate of Jekyll Island were 1 m and 2 m during 1957-1999.

The north end of Jekyll Island has had a long history of erosion, and is where the most severe recession has taken place. Two human activities contributed to this problem. Since the dredging of St. Simons Sound ship channel in 1909, it is annually dredged to allow deep-draft container ships to enter Brunswick Harbor. The channel swallows much of the sand drifting southward in the alongshore currents from St. Simons Island and the other islands to the north. Most of the sand sinks into the ship channel leaving little sand for shoal development and nourishment of Jekyll Island's northern beaches. An additional factor was President Lyndon Johnson's order for the emplacement of a seawall composed of huge granite boulders known as the Johnson Rocks at the south end of St. Simons Island in 1964. While it lessened the landward erosion of southern St. Simons Island, it exacerbated the shoreline erosion problem at northern part of Jekyll Island (Lenz, 1999). As seawalls block shoreline retreat, the beach is squeezed against these obstacles, which causes it to narrow and leads to a reduction in sand supply to adjacent beaches.

However, the results from this research indicate that Jekyll Island lost significantly fewer beaches annually, and the maximum recession rates were statistically smaller than those of

Sapelo Island during 1954-1974 and 1974-1993. This is because erosion control measures were implemented to protect beaches on Jekyll Island. A rock seawall of granite boulders was built in mid 1960s from about 2-km south to the fishing pier to just north of the Convention Center to offset the erosion (see Figure 6.2). A seawall is a structure built on a beach, parallel to the shoreline, designed to protect buildings from the action of waves, but such armoring can be visually unpleasant for a recreational beach. Beach nourishment and dune building were implemented on the beach south to the Convention Center (see Figure 6.3). This area was assaulted by beach-lovers whose walking up and down the dunes caused great erosion. Signs to remind tourists to keep off dunes, like Figure 6.4, can be seen near the beach. Dune plants hold the sand in place, and when they are killed, the sand is liberated, causing a domino effect. Tons of freed sand migrated southward on Jekyll Island. In 1983, a beach restoration project formed new primary dunes with bulldozed sand, installed snow fences, planted sand-trapping plants, and built two boardwalks over the dunes (Lenz, 1999). Conversely, Sapelo Island and the Blackbeard Island to its north remain in a pristine state.

The annual mean erosion rates of Jekyll and Sapelo islands are not statistically different between 1954 and 1999 according to this study. This is because the 1999 lidar image does not cover the whole northern end, where most severe recessions occur. Shorelines traced from other images starts from the fishing pier on the northern tip.

Coastal managers or planners are equally concerned about the volumetric changes of a recreational beach, such as that on Jekyll Island. The most accurate way to compute the volumetric change is by comparing beach profiles obtained from field surveys that include the nearshore areas. In the absence of such information, an empirical relationship can be applied to calculate the volume of change: one foot of beach erosion perpendicular to the beach is

equivalent to one cubic yard of material per linear foot of beach (U.S. Army Corps of Engineers, 1964). The mean accretion rate of Jekyll Island during 1957 and 1999 is 3 m per year, therefore, the amount of yearly deposition along the 12-km seaward beach is 324,000 m^3. In the same manner, the amount of yearly erosion and yearly net change were computed to be 108,000 m^3 and 216,000 m^3. The net gain on Jekyll Island could be largely attributed to the rock seawall and the beach nourishment project.

Inaccuracy in the data has several possible causes. First, positional errors exist in source data, such as shrinkage or distortion of 1974 paper aerial photograph sets. Second, errors are present in aerial photograph image rectification. Even though the rectification eliminates the radial lens distortion and tilt displacement, it does not correct the displacement caused by relief. Fortunately, the Atlantic barriers islands are relatively flat, so that distortion due to relief displacement is usually negligible (Crowell *et al.* 1991). In addition, though anthropogenic features are preferred as GCPs rather than natural points, in some cases cultural features, such as road intersections or low-relief building corners, are lacking. This is especially true for Sapelo Island, as it remains in a pristine state. Less reliable points, such as river meanders or edge of water bodies, are used as reference points under such conditions. Third, inaccuracy is introduced during shoreline interpretation. For instance, shoreline position maybe incorrectly interpreted due to poor image quality or interpretation error. Last, the exact flight time of 1974 aerial photograph acquisition and 1993 DOQQs are unavailable. Because the exact time of photograph acquisition affects the calculation of real-time tidal heights, there are possible errors in the estimation of tidal heights. However, the estimated acquisition time (11:30 am) is well verified by the flight specifications and feature's shadow size and direction on the photographs. Besides, the largest tidal height difference between 10:00 am and 11:30 am for Jekyll and Sapelo islands

is 73 cm. The tidal heights for the two islands at 10:00 am are summarized in Table 6.1. The differences are negligible compared with the average distance of shoreline movement during the study time periods. Because the inaccuracy of map projection, aerial photograph rectification and misalignment is controlled less than 2.4 m, 2 m and 4 m, and the biggest error in tidal height is 0.73 m, the largest positional error from the input data is about 9 m. This combined error is much smaller than the smallest of the average shoreline positional change which is 38 m, besides, only 5% of the sample locations experienced less than 10-m positional change during the study periods. Hence, the results are not affected appreciably by composite error.

The Metric Mapping ArcView extension is a powerful tool for analyzing and displaying digital shoreline data from various sources. Users can construct transects with user-specified interval, measure distance of movement and compute change rate with EPR or LR methods. The extension also allows users to list results in tabular format and graphically represent those data. Because Metric Mapping is embedded in ArcView, its function is easy to expand by writing codes in Avenue when additional tools are needed. Users also have the full power of ArcView to perform their analysis and tasks.

This research differs from the previous work in several significant ways. In most previous studies a surrogate for shoreline was used. As Dolan *et al.* (1980) concluded that the boundary between wet sediment and dry sediment is the most commonly used surrogate for shoreline position as it approximates the mean high water level (MHWL). Generally, this line can be recognized by a change from dark to light tones on images. Even though this boundary is less susceptible to daily changes in ocean water levels than the water line, there is still a discrepancy between this proxy and the true position of MHWL. Such differences can be substantial especially in tide-dominated settings, such as the Georgia coast. In addition, this line

often appears as a gradational zone of change. In this research shorelines from multiple years were referenced to the same tidal datum. For example, real-time water lines were first interpreted and delineated from aerial photographs and DOQQs, and then registered to MLLW based on the tide tables. It eliminated tidal influence by comparing positions of the same line---MLLW in different years.

Historical rates of shoreline change for Georgia's barrier islands are lacking in quantity and quality. The state of Georgia only implemented its Coastal Management Program under NOAA's National Coastal Zone management Program in 1998, yet little has been done to regularly map the shoreline, thus up-to-date information on average annual recession rates are lacking. Such fundamental information is essential for coastal planning and is crucial to Georgia coast in particular, as the coastal area is faced with serious erosion problems. Obtaining statistically valid information on the directions and rates of coastline change fills an existing knowledge void for the Georgia coast.

Among limited research on the Georgia coast, the majority focused on individual developed islands and inlets, generally related to coastal engineering, ship channel dredging projects or beach nourishment (Frey and Howard, 1988). Few works have been done on the coastline of undeveloped barrier islands, let alone on the comparison of them. These federal or state government owned islands remain pristine with minimal development and are not in urgent need of updated information on coastline change due to lack of infrastructure at risk from coastal erosion (Foyle, 2000). But these undeveloped islands provide contrast to the developed ones within the same physical settings in coastal response. This project compared the shoreline change pattern, erosion rate and accretion rate of Jekyll and Sapelo islands during the last four decades. Such quantified information on the coastline change is helpful to understand complex

coastal systems and the effects of partly engineered systems on barrier islands. Thus, it provides valuable inputs to future coastal erosion mitigation.

GIS simplifies the compilation of shoreline from a variety data types by allowing transformation to a common projection, coordinate system, datum and ellipsoid (Moore, 2000). The 1999 shorelines were extracted from a set of lidar images, a technology that offers an exciting new way to efficiently document and measure shoreline change. With traditional beach surveying methods, data are collected in a transect seaward from a benchmark. It is labor intensive to cover a large area of beach with conventional beach surveying methods. Conversely, lidar techniques are proving to be a more efficient and less costly way of collecting shoreline topography, provided that sub-tidal data are not needed. The data set provides a horizontal accuracy of less than 50 cm and a vertical accuracy of ±15 cm. In addition, it offers accurate data in locations and conditions where traditional surveying techniques cannot be applied. Many coastal states may benefit from this technology as it is a helpful aid in understanding how, when, and where erosion and accretion are occurring along the coastline.

Coastal areas are intensely used areas settled by humans. Many countries show above-average concentrations of population near the coast and two-thirds of the world's largest cities are located on coasts (Masselink and Hughes, 2003). Shoreline change study helps to understand how the coastline respond to natural processes and provides useful data on predicting the future trend. In addition to creating a scientific basis for shoreline monitoring and management, coastline change research also offers useful information on the impacts of engineering structures on erosion. This is needed to understand the consequences that induced by placement of a specific type of structure (Frey and Howard, 1988). Such scientific understanding and predictive capability can enable coastal hazard mitigation to move from a reactive stance to a more

proactive decision making process, and hence minimize negative impacts to the environment, and reduce potential economic and human losses (Bush *et al.* 2002).

Given the dynamic nature of the coastal region and complexity of coastline change, quantifying shoreline change still has some challenges (NOAA, 2002). First, such studies require the researchers not only be familiar with most updated methodologies and measurement theory, but also to have a comprehensive understanding of the capture of historical shoreline data. Second, a shoreline change analysis is not strictly defined yet and a lack of standardization exists in several aspects. For example, what line on the ground or image is the most appropriate indicator of shoreline position? Guidelines are needed to assist coastal communities in choosing a consistent indicator. There are a number of approaches to quantify change, and there is no single widely accepted method so far. Universal definitions of the time scales are needed, such as how many years is considered short-term or long-term, and under what circumstances they should be used. Third, advancements in GPS, GIS and lidar have benefited coastline change research. The challenge for the coastal community is to develop data structures and algorithms to apply the integrated method, to produce high-resolution topographic image in the same reference frame, and construct accurate tidal models for the coastal region. Last, the biggest challenge is how to best quantify and present shoreline change data and convert good science into policies with long-term benefits for coastal communities. It requires cooperation among federal agencies, state or local governments and research units to make this conversion possible.

Table 6.1 Computed tidal heights for Jekyll Island and Sapelo Island at 10:00 am

	Jekyll		Sapelo	
Year	1974	1993	1974	1993
Height (cm)	107	116	186	66

Figure 6.1 Coastal erosion at the north end of Jekyll Island, Georgia

Figure 6.2 The rock seawall on Jekyll Island, Georgia

Figure 6.3 Sand dunes on Jekyll Island, Georgia after beach restoration

Figure 6.4 A sign reminding tourists to keep off dunes

References

Alkaff, H.E., 1997, *Spatial and temporal changes in wetlands and beaches of the Sapelo Island complex, Georgia.* Master Thesis, The University of Georgia

Anders, F.J. and Byrnes, M.R., 1991, Accuracy of shoreline change rates as determined from maps and aerial photographs, *Shore and Beach*, 59(1), 17-26

Ashry, M.R. and Wanless, H.R., 1967, Shoreline features and their changes, *Photogrammetric Engineering,* 33(2), 185-189

Bates, R.L. and Jackson, J.A. (editors), 1984, *Dictionary of geological terms*, 3rd edition, Anchor Press / Doubleday, Garden City, NY, 316

Brown, P.J., 1977, Variations in South Carolina coastal morphology, *Southeastern Geology*, 18, 259-264

Bush, D. M., Alexander, C. R., Foyle, A. M., Langley, S. K., Henry, V. J., Jackson, C. W. and Wilson, C., 2002, Quantitative shoreline change analysis of the Georgia coast from aerial photograph, Retrieved July 17, 2003 from http://gsa.confex.com/gsa/2002NC/finalprogram/abstract_31643.htm

Carter, V., 1978, Coastal wetlands: role of remote sensing, *Proceedings of Symposium on Technical, Environmental, Socioeconomic and Regulatory Aspects of Coastal Zone Management, held in San Francisco, California* (New York: ASCE) 1261-1284

Chen, L.C. and Rau, J.Y, 1998, Detection of shoreline changes for tideland areas using multi-temporal satellite images, *International Journal of Remote Sensing,* 19(17), 3383-3397

Chen, L.C. and Shuyu, C.C., 1995, Automated extraction of shorelines from optical and SAR image, *Proceedings of the 1998 Asian Conference on Remote Sensing, held in Manila, Philippine,* Poster session 3

Cracknell, A.P. 1999, Remote sensing techniques in estuaries and coastal zones-an update, *International Journal of Remote Sensing*, 19(3), 485-496

Crowell, M., Leatherman, S.P., and Buckley, M.K., 1991, Historical shoreline change: Error analysis and mapping accuracy, *Journal of Coastal Research,* 7(3), 839-852

Coastal Georgia Regional Development Center, Retrieved July 17, 2003 from http://www.coastalgeorgiardc.org/overview.html

Dolan, R., and Davis, R.E., 1992, An intensity scale for Atlantic coast northeast storms, *Journal of Coastal Research*, 8(4), 840-853

Dolan, R., Fenster, M.S., and Holme, S.J., 1991, Temporal analysis of shoreline recession and accretion, *Journal of Coastal Research*, 7(3), 723-744

Dolan, R., Hayden, B.P., Rea, C.C., and Heywood, J., 1979, Shoreline erosion rates along the middle Atlantic coast of the United States, *Geology*, 7, 602-606

Dolan, R., Hayden, B.P., May, P., and May, S., 1980, The reliability of shoreline change measurements from aerial photographs, *Shore and Beach*, 48(4), 22-29

Donoghue, D.N.M., Thomas, D.C.R., and Zong, Y., 1994, Mapping and monitoring the intertidal zone of the east coast of England using remote-sensing techniques and a coastal monitoring GIS, *Marine Technology Society Journal*, 28(2), 19-29

Fisher, J.J. and Simpson, E.J., 1979, Washover and tidal sedimentation rates as environmental factors in development of a transgressive barrier shoreline, *In: Leatherman, S.P., (ed.), Barrier Islands*, New York: Academic P, 127-148

Foyle, A.M., 2000, Coastal change in Georgia: State of knowledge and geo-research needs, Retrieved October 11, 2003 from http://www.personal.psu.edu/faculty/a/m/amf11/coastal-change.htm

Frey, R.W. and Howard, J.D., 1988, Beach and beach-related facies, Holocene barrier islands of Georgia, Geology 125, 621-640

Frihy, O.E., Nasr, S.M., Hattab, M.M.EL and Raey, M.E.L., 1994, Remote sensing of beach erosion along the Rosetta Promontory Northwestern Nile Delta, Egypt, *International Journal of Remote Sensing,* 15 (8), 1649-1660

Hiland, M.W., Byrnes, M.R., McBride, R.A., and Jones, F.W., 1993, Change analysis and spatial information management for coastal environments, *Microstation Manager*, March, 58-61

Inman, D.L. and Brush, B.M., 1973, The Coastal challenge, *Science*, 181, 20-32

Jekyll Island, Retrieved April 6, 2004 from http://www.jekyllisland.com

Krabill, W., Abdalati, W., Frederick, E., Manizade, S., Martin, C., Sonntag, J., Swift, R., Thomas, R., Wright, W. and Yungel J., 2000, Greenland ice sheet: High-elevation balance and peripheral thinning, *Science*, July 21, 428-430

Leatherman, S.P., 1983, Shoreline mapping: A comparison of techniques, *Shore and Beach*, 51, 28-33

Lenz, R.J., 1999, *Longstreet highroad guide to the Georgia coast and Okefenoke*, Longstreet Press, 255-271

Li, R.X., Liu, J.K. and Felus, Y., 2001, Spatial modeling and analysis for shoreline change detection and coastal erosion monitoring, *Marine Geodesy*, 24, 1-12

Lillesand, T.M. and Kiefer, R.W., 2000, *Remote sensing and image interpretation*, 4th edition, John Wiley & Sons, Inc. 165-166

Liu, J.K., 1998, Developing GIS applications in analysis of responses to Lake Erie shoreline changes, Master Thesis, Department of Civil and Environmental Engineering and Geodetic Science, The Ohio State University

Massenlink, G. and Hughes, M.G., 2003, *Introduction to coastal processes & geomorphology*, 1st edition, Oxford University Press Inc. 21, 45, 307

McBeth, F.H., 1956, A method of shoreline delineation, *Photogrammetric Engineering,* 22, 400-405

Moore, L.J., 2000, Shoreline mapping techniques, *Journal of Coastal Research*, 16 (1), 111-124

Morton, R.A., 2003, An overview of coastal land loss: With emphasis on the Southeastern United States, USGS Open File Report 03-337, Retrieved March 26, from http://pubs.usgs.gov/of/2003/of03-337/intro.html

Nash, G.N., 1977, Historical changes in the mean high water shoreline and nearshore bathymetry of south Georgia and north Florida, The University of Georgia M.S. thesis in geology

NOAA, 2002, Challenges for the future, *Proceedings of Shoreline Change Conference, held in Charleston, South Carolina,* Retrieved March 26, from http://www.csc.noaa.gov/shoreconf/challenges.html

Philipson, W.R. (editor-in-chief), 1997, *Manual of photographic interpretation*, 2nd edition, American Society for Photogrammetry & Remote Sensing, 94-95

Revell, D.L., Komar P. D. and Sallenger A.H., Jr., An application of Lidar to analyses of El Niño erosion in the Netarts littoral cell, Oregon, *Journal of Coastal Research,* Vol. 18, No. 4, 792-801

Schoettle, T., and Johnson, C., 1987, *A field guide to Jekyll Island*, University of Georgia Printing Program, 3-7

Scott, J., Reed, M. and Moore L., 2002, Using Landsat 7 images to derive a land-water boundary in Southern Louisiana, technical report, Mid-Continent mapping Center, U.S. Geological Survey

Shalowitz, A.L., 1964, Shore and sea boundaries, volume 2, U.S. Department of Commerce, Publication 10-1, U.S. Govt. Printing Office, Washington, D.C., 749

Stafford, D.B., 1971, An aerial photographic technique for beach erosion surveys in North Carolina, Washington DC: U.S. Army Corps of Engineers. Coastal Engineering Research Center, Technical Research Center, Technical Memorandum. NO.36, 115

Stafford, D.B. and Langfelder, J., 1971, Air photo survey of coastal erosion: *Photogrammetric Engineering*, 37, 565-575

Stockdon, H.F., Sallenger, A.H.Jr, List, J.H. and Holman R.A., 2002, Estimation of shoreline position and change using airborne topographic Lidar data, *Journal of Coastal Research*, 18 (3), 502-513

Stokkom, H.T.C., Stokman, G.M. and Hovenier, J.W., 1993, Quantitative use of passive optical remote sensing over coastal and inland water bodies, *international Journal of Remote Sensing*, 14, 541-563

Taylor, L., Harding, J., Henry, V.J., Kelly, J. and Trulli, H., 1995, Assessment of environmental research and nonmineral resources offshore Georgia, Georgia Department of Natural Resources, Environmental Protection Devision, Georgia Geologic Survey Project Report 21, 346

The University of Georgia Marine Institute, A Sapelo Island eHandbook, 2001, Retrieved July 17, 2003 from http://www.arches.uga.edu/~sapelo/

U.S. Army Corps of Engineers, 1964, Outer banks between Ocracoke inlet and Beaufort inlet, Combined Report on an Interim Hurricane Survey and Cooperative Beach Erosion Control Study, U.S. Army Engineer District, Wilmington, North Carolina

Wang, Y., and Koopmans, B.N., 1993, The topographic mapping of the tidal flats using remote sensing and GIS techniques: A case study in the Wadden Sea area, Netherland, *Proceedings of International Symposium of Operationalization of Remote Sensing*, 193-203

Welch, R., Remillard, M., and Alberts, J., 1992, Integration of GPS, remote sensing, and GIS techniques for coastal resource management, *Photogrammetric Engineering and Remote Sensing*, 58, 1571-1578

White, S.A. and Wang, Y., 2003, Utilizing DEMs derived from Lidar data to analyze morphologic change in the North Carolina coastline*, Remote Sensing of Environment*, 85, 39-47

Zhang, Keqi and Robertson, W., 2001, Historical shoreline mapping and analysis with metric mapping, *Proceeding of the 2nd Biennial Coastal GeoTools Conference, held in Charleston, South Carolina*, *January 8-11, 2001*